REPORT NO. FRA/ORD-81/49

IMPROVEMENT IN MAGNETIC TECHNIQUES FOR RAIL INSPECTION

George J. Falkenbach
David J. Kooger
Robert P. Meister

Battelle Columbus Laboratories
505 Columbus Avenue
Columbus OH 43201

JUNE 1981

FINAL REPORT

DOCUMENT IS AVAILABLE TO THE PUBLIC
THROUGH THE NATIONAL TECHNICAL
INFORMATION SERVICE, SPRINGFIELD,
VIRGINIA 22161

Prepared for

U.S. DEPARTMENT OF TRANSPORTATION
FEDERAL RAILROAD ADMINISTRATION
Office of Research and Development
Washington DC 20590

Technical Report Documentation Page

1. Report No.	2. Government Accession No.	3. Recipient's Catalog No.
FRA/ORD-81/49		

4. Title and Subtitle	5. Report Date
IMPROVEMENT IN MAGNETIC TECHNIQUES FOR RAIL INSPECTION	June 1981
	6. Performing Organization Code: DTS-733
7. Author(s): G.J. Falkenbach, D.J. Kooger, R.P. Meister	8. Performing Organization Report No.: DOT-TSC-FRA-81-14
9. Performing Organization Name and Address: Battelle Columbus Laboratories* 505 Columbus Avenue Columbus OH 43201	10. Work Unit No. (TRAIS): RR931/R9326
	11. Contract or Grant No.: DOT-TSC-1244-1
12. Sponsoring Agency Name and Address: U.S. Department of Transportation Federal Railroad Administration Office of Research and Development Washington DC 20590	13. Type of Report and Period Covered: Final Report Aug. 76 - Dec. 77
	14. Sponsoring Agency Code: RRD-31

15. Supplementary Notes

*Under contract to: U.S. Department of Transportation
Research and Special Programs Administration
Transportation Systems Center
Cambridge MA 02142

16. Abstract

Current inspection of rail for internal defects is carried out by ultrasonic and/or magnetic techniques. This report covers work directed toward advancing present-day magnetic technique for inspecting rail for internal flaws. The major emphasis was placed on improving the speed and detectability of current techniques.

Experimental work was performed directed toward determining where and how improvements can be made with existing equipment and techniques. The three major areas investigated for improvement were 1) magnetization 2) flaw sensors and 3) signal processing.

A series of full-scale dynamic experiments were conducted with several magnetic configurations on a test track containing a high concentration and variety of actual rail defects. Certain magnetic flaw detection techniques were demonstrated for several types of rail defects and identification/characterization methods were modeled for a hypothetical system.

17. Key Words	18. Distribution Statement
-Track, Flaw, Ultrasonic, Magnetic Inspection, Automatic Data Processing Rail, Nondestructive Testing	DOCUMENT IS AVAILABLE TO THE PUBLIC THROUGH THE NATIONAL TECHNICAL INFORMATION SERVICE, SPRINGFIELD, VIRGINIA 22161

19. Security Classif. (of this report)	20. Security Classif. (of this page)	21. No. of Pages	22. Price
Unclassified	Unclassified	104	

Form DOT F 1700.7 (8-72) Reproduction of completed page authorized

PREFACE

This report presents the results of a program dealing with investigation of improvements that are possible in advancing present-day magnetic techniques for rail inspection, whether to be operated as an independent system or in conjunction with and supplementary to an ultrasonic rail inspection system. The report was prepared by Battelle's Columbus Laboratories under Contract No. DOT-TSC-1244 from Transportation Systems Center and was sponsored by the Office of Research and Development of the Federal Railroad Administration. Mr. Harry Ceccon was the technical monitor for this contract. The cooperation, suggestions, and assistance provided by Mr. Ceccon are gratefully acknowledged.

This program could not have been carried out without the cooperation of: Mr. D. H. Stone, Director - Metallurgy, Association of American Railroads (AAR), who graciously permitted use of their test track; Mr. A. Gene (Tex) Payne, AAR Detector Car Supervisor, for his relentless assistance in providing for and helping to conduct the field tests; Mr. H. W. Copeland, Inspector - Detector Car, Southern Railway, for use of magnetic detector car parts; and to consultants Mr. Payne, Mr. W. G. Brazitis (retired) and Mr. J. A. Franks, American Rail Testing, for their most able assistance in providing intimate first-hand knowledge of magnetic detection principles and practice.

Approximate Conversions to Metric Measures

Symbol	When You Know	Multiply by	To find	Symbol
	LENGTH			
in	inches	2.5	centimeters	cm
ft	feet	30	centimeters	cm
yd	yards	0.9	meters	m
mi	miles	1.6	kilometers	km
	AREA			
in^2	square inches	6.5	square centimeters	cm^2
ft^2	square feet	0.09	square meters	m^2
yd^2	square yards	0.8	square meters	m^2
mi^2	square miles	2.6	square kilometers	km^2
	acres	0.4	hectares	ha
	MASS (weight)			
oz	ounces	28	grams	g
lb	pounds	0.45	kilograms	kg
	short tons (2000 lb)	0.9	metric ton	t
	VOLUME			
tsp	teaspoons	5	milliliters	ml
Tbsp	tablespoons	15	milliliters	ml
fl oz	fluid ounces	30	milliliters	ml
c	cups	0.24	liters	l
pt	pints	0.47	liters	l
qt	quarts	0.95	liters	l
gal	gallons	3.8	liters	l
ft^3	cubic feet	0.03	cubic meters	m^3
yd^3	cubic yards	0.76	cubic meters	m^3
	TEMPERATURE (exact)			
°F	Fahrenheit temperature	5/9 (after subtracting 32)	Celsius temperature	°C

Approximate Conversions from Metric Measures

Symbol	When You Know	Multiply by	To find	Symbol
	LENGTH			
mm	millimeters	0.04	inches	in
m	meters	3.3	feet	ft
m	meters	1.1	yards	yd
km	kilometers	0.6	miles	mi
	AREA			
cm^2	square centimeters	0.16	square inches	in^2
m^2	square meters	1.2	square yards	yd^2
km^2	square kilometers	0.4	square miles	mi^2
ha	hectares (10,000 m^2)	2.5	acres	
	MASS (weight)			
g	grams	0.035	ounces	oz
kg	kilograms	2.2	pounds	lb
t	metric ton (1,000 kg)	1.1	short tons	
	VOLUME			
ml	milliliters	0.03	fluid ounces	fl oz
l	liters	2.1	pints	pt
l	liters	1.06	quarts	qt
l	liters	0.26	gallons	gal
m^3	cubic meters	35	cubic feet	ft^3
m^3	cubic meters	1.3	cubic yards	yd^3
	TEMPERATURE (exact)			
°C	Celsius temperature	9/5 (then add 32)	Fahrenheit temperature	°F

TABLE OF CONTENTS

LIST OF FIGURES

LIST OF FIGURES (Continued)

LIST OF TABLES

1. EXECUTIVE SUMMARY

Magnetic rail inspection techniques are based on the sensing of perturbations in the magnetic field emanating from a magnetized or electrified rail. The magnetic field perturbations are caused by material and structural variations within the rail, especially in the surface of the railhead. The entire thrust of magnetic rail inspection is to clearly distinguish between the magnetic field perturbations associated with critical flaws such as transverse fissures and those perturbations associated with extraneous noncritical flaws such as slight changes in metallurgical composition of the rail head. The three generic magnetic inspection techniques are residual magnetization, applied magnetization, and induced magnetization. Each of these generic inspection techniques utilizes a different aspect of the electrodynamic and/or magnetodynamic interaction of electric currents and/or magnetic fluxes with the rail structure.

The general objective of this program was to advance the state-of-the-art of present-day magnetic rail inspection systems by determining where and how improvements can be made in any aspect of the existing techniques and equipment in use. Technical areas addressed include:

- Improving magnetization within the rail
- Investigating and developing improved sensors
- Considering more-advanced signal processing methods leading to automated detection and classification on a real-time basis, without the need for operator involvement.

The AAR residual magnetic technique was used as a baseline from which technical areas such as improving magnetization, developing improved sensors, and studying more advanced signal processing methods for real-time application were addressed.

A series of full-scale dynamic experiments were conducted with several apparatus configurations on a test track containing a high concentration and variety of actual rail defects.* Certain flaw detection

*A detailed listing of the flaws in the AAR test track is given in Appendix A.

techniques were demonstrated for several types of rail defects, and flaw identification/characterization methods were modeled and a hypothetical system conceptualized.

A total of thirty test runs were conducted during the program on the AAR test track at low speeds using a full-scale test apparatus. The test apparatus was configured first to duplicate the residual magnetic technique as a baseline. Other configurations tested were based on the applied (active) magnetic technique. An AAR Model-8 magnet structure, capable of up to 18,500 ampere-turns, magnetomotive force, was used for all the residual and some of the longitudinal applied magnetic tests. A pair of small magnets, with up to 8,000 ampere-turns, supplied the magnetizing field for the other longitudinal and all the transverse applied magnetic configurations. Magnet pole spacings used were 2-1/2 ft for the residual magnetic method and were varied from 4-1/4 to 11-1/2 ft for the longitudinal applied method. The track dynamics of the test apparatus were not satisfactory at the higher speeds ($\sim$15 mi/h) due to an excessively rigid mechanical design; as a result, the test data obtained were marked by considerable noise due to detector carriage bounce.

This program involved the evaluation of new methods for magnetizing the rail, e.g., methods which presently are not used in the United States, including two basic configurations for implementing the applied magnetic method, namely longitudinal and transverse magnetization. The applied magnetic method was found potentially superior to the residual method. Use of a longitudinal magnetic field applied with an 11-1/2-ft pole spacing led to a long-term retained field in the railhead of >1 kilogauss at 15 mi/h, thus suggesting that operational speeds of 40 mi/h are possible with appropriate sensors. Depth of penetration of the magnetic field increased dramatically for larger pole spacings, as did the residual field.

Sensors comprising the standard AAR pickup coils as well as an array of Hall effect sensors, scanning the same railhead region as the AAR coils, and an eddy current probe were used. Test speeds were run from 4 to 15 mi/h (6.5 to 24 km/h). Data were taken on up to 12 sensors per run with a few sensors being common to all runs. The instrumentation was operated with a greater sensitivity than customarily done under regular magnetic rail

inspection conditions. The presence of many previously unknown or undocumented flaws, which were subsequently confirmed by other test techniques, were thus "discovered".

Pickup coils wound on a magnetic core oriented transverse to the plane of a rail defect were found to be the most sensitive sensors to use. The key to magnetic detection of rail flaws appears to be intimately related to the rise and fall times of the leakage flux signals. If coils are differentially wound a better signal-to-noise ratio results. A Hall element is less sensitive than a pickup coil but it can be made to have a smaller spatial resolution by virtue of its much smaller size. Also, the Hall element does not suffer the speed dependency like a coil does due to lack of high-frequency signal response or L/R time constant effects. It is most sensitive to transverse defects when it is lying in a plane parallel and quite close to the railhead surface. The Hall element, when centered vertically above the railhead, is a good detector of vertical splits in the railhead; however, no direct comparison was made with an ultrasonic system configured to locate VSH.

A minicomputer was used to model a variety of signal analysis procedures to aid in identifying criteria for flaw detection and characterization, as well as false signal rejection. The procedures evaluated that were found successful included such schemes as differentiation, scaling, thresholding (baseline clipping), and modulation. Major emphasis was placed on discovering ways to enhance flaw/detection as well as to reduce the effect of extraneous signals such as from the joint bar regions. With respect to flaw characterization, however, a pattern recognition system is necessary. No simple analog method is available to implement a system of the type required here and a digital approach is necessary. Due to a lack of sufficient flaw documentation and time, it was only possible to conceptualize a flaw indication system and to define how the flaws can be classified by an automatic means. It was not possible to attempt design, building, and tryout of such a system.

1.1 Conclusions

Magnetic rail flaw detection techniques have been rather broadly investigated and the following points emerge:

1. The current speed limitation in the AAR residual magnetism technique is not due to the inability to induce a strong enough magnetic field, but rather the lack of sufficient high-frequency response and discrimination in the coils because of the use of laminated steel cores. This could be circumvented by employing ferrite cores or using Hall elements with additional signal electronics in place of coil sensors.
2. Longitudinal applied (active) magnetization with an 11-foot-long inverted U-shaped magnet was shown to provide improved flux penetration for inspection at higher speeds. Magnetic flux sensors were placed between the poles, i.e., within the active region of the magnet. Sufficient magnetizing fields have been applied for this configuration to be demonstrated at approximately 25 mi/h, and it shows potential for working at 40 to 50 mi/h. The most sensitive sensors used are pickup coils which respond to the derivative of leakage flux fields at defects, but these would suffer a loss in sensitivity at these higher speeds, as noted above.
3. The only way to reduce the size and weight of the magnetizing structure is to reduce the airgap at the magnetizing pole faces; this is difficult for higher speeds.
4. The payoff in this program has been in discovering successful decision algorithms to aid in flaw detection, location, and identification. By utilizing digital signal processing routines such as differentiation, thresholding (baseline clipping), scaling, and comparing, procedures have been demonstrated which successfully detect and identify various classes of flaws. Such procedures reduce the noise levels in the signal records, thus relieving the operator of much burden as far as workload is concerned. A necessary key in this effort has been the realization that reliability is greatly enhanced with the use of a voting network. But, in spite of the above, more work is required to discriminate flaws from shelling and some engine burns which have definite flaw-like signatures.

5. Discriminating between flaw types is not accomplished by analyzing the outputs of single sensors, but rather by which one of the sensors detects the flaw. For example, if the sensors observing the gage corner of the rail see a flaw with a "schmoo" response and the other sensors from midrail out see nothing, then it is quite likely that the flaw is a detailed fracture. Similarly, other patterns can be discerned that uniquely identify the other types of flaws.
6. Although a flaw characterization system was conceptualized which would specify the type of flaw detected, it is a more difficult problem to characterize the size of a flaw any more precisely than small (<20%) or large (>40%).
7. A limited investigation was carried out on flaws within the joint bar regions. It has been possible to see some defect indications in the railhead up to within 1-2 inches of the rail ends. Although there has been no confirmation of these suspected flaws from any AAR chart records or documentation, there is no question as to their existence. This is mainly the result of conducting the experiments with higher than usual sensitivity which has resulted in the ability to analyze raw signals in considerably more detail. With further development of the several signal processing routines employed, it should be possible to detect by magnetic means transverse defects in the joint regions to within about 1 inch of the end of the rail.
8. In addition to improving the reliability of the detection system, a means has been found to automatically identify rail joints. The output from a sensor coil is fed into a low-pass filter and is thresholded. This signal can then be applied to a wave shaper with the final output appearing as a pulse, the duration of which is the length of the joint bars.
9. Insufficient experimental results were obtained to fully evaluate the potential of eddy current detectors as indicators in rail flaw detection. Although such a sensor has potential for identifying/locating nonharmful surface anomalies such as engine burns, the use of an absolute probe coil in these experiments rather than a differential coil (probe or saddle type) was unfortunate. The "liftoff" signal -- a function of coil face to rail surface separation -- was much more sensitive to mechanical/physical conditions than the quadrature signal. Further study and experimentation are in order.

1.2 Recommendations

Based on the work conducted during this program and the results obtained, it is recommended that an additional effort be expended to:

1. Complete detail design, build, and operate the flaw detection system as conceptualized. The system can be "operated" against the data tape created during this program, but a more realistic proof would be obtained if the system were operated in a real railroad environment along with other operating rail flaw inspection equipment.
2. Study, design, and build prototype coil sensors similar to the AAR pickup coils but having ferrite cores instead of laminated steel so as to allow operation at higher speeds.
3. Perform additional experiments with eddy current sensors having greater sensitivity to nonharmful surface anomalies such as engine burns, shelling, and the like.

2. INTRODUCTION

Inspection of railroad trackage has been improved over the last ten years as a result of continuing advancements in the application of ultrasonic techniques. Ultrasonic equipment was first used for rail inspection principally to augment magnetic rail flaw detection equipment investigated and developed by Dr. Sperry some fifty years ago.[1]* That scheme is herein referred to as the "direct-current-by-contact" technique or "induction magnetic" technique. Before Sperry's work, the Bureau of Standards had undertaken a program to determine the cause of the common rail flaws which came to be known as transverse fissures. They also aided in developing a magnetic method suitable to locate such internal defects in rail before catastrophic failures occurred in service which came to be known as the "residual magnetic" technique. In recent years, use of ultrasonics as a rail inspection technique has gained wider acceptance. Although ultrasonics appears to have great potential for rail inspection systems, further development is required before thorough inspection can be performed by ultrasonics alone. In addition, since ultrasonic inspection devices are insensitive to certain flaws, magnetic inspection methods are necessary to complement ultrasonic systems.

The application of ultrasonic methods has led to more thorough rail inspection by offering the additional capabilities of inspecting for web defects, such as bolt-hole cracks at joints, and head and web separations at rail ends. On the other hand, ultrasonic rail inspection methods require not only a fluid couplant but also very critical and precise mechanical alignment, whereas magnetic inspection methods do not. The most serious drawback of current ultrasonic methods is the inability to inspect the upper outmost corners (both gage and field sides) of the railhead area.[2]** Even by employing ultrasonic beams in a pitch-catch mode between coupling wheels separated to accomodate multiple-bounce shallow-entering beams, it is not reasonably assured

---

* A good general source of information on rails, defects, and testing can be found in Reference 1.

** The complementary nature of magnetic and ultrasonic inspection systems is evident from Reference 2.

that the upper gage-side and field-side corners of the railhead can be inspected for defects. Such a complex skewed angle-beam transmission path does, however, cover the lower railhead fillet areas near the web as well as the lower gage- and field-side corners. Also, ultrasonic methods have difficulty detecting defects under surface anomalies. Since magnetic inspection of rail in the United States today is confined to unobstructed railhead areas only -- it is not used to inspect rail within joint bar regions, switches, frogs, nor can it inspect the web or base -- ultrasonic techniques complement magnetic techniques well for inspecting for defects in such places.

In spite of the increased attention given in recent years to ultrasonic inspection of rail, magnetic methods offer certain advantages. Some experienced rail inspectors believe that magnetic systems are more reliable for detecting and identifying transverse fissures because of their straightforward operating concept, relatively simple electronic circuitry, and minimal environmental effects. On the other hand, magnetic techniques have some defficiencies in the present state of development, such as limits imposed by the existing physical separation of the magnet poles or of the current-contacting brushes. Rail surface conditions sometimes give anomalous defect indications. Joint bars make it difficult to discover defects in the joint area, and penetration of the magnetic field (or current) decreases with increasing speed, resulting in a loss of sensitivity to internal defects. These deficiencies exist today because improvements made possible by recent advances in solid-state electronics, small dedicated computers, and sophisticated signal processing routines have not been considered. Thus it seems prudent to search for a combined magnetic-ultrasonic system that can offer the best features of both while having none of the disadvantages of either.

The general objective of this program was to advance the state-of-the-art of present-day magnetic rail inspection systems by determining where and how improvements can be made in any aspect of the existing techniques and equipment in use. Technical areas addressed include:

- Improving magnetization within the rail
- Investigating and developing improved sensors
- Considering more-advanced signal processing methods leading to automated detection and classification on a real-time basis, without the need for operator involvement.

3. REVIEW OF MAGNETIC RAIL INSPECTION TECHNIQUES

Magnetic rail inspection techniques are based on the sensing of perturbations in the magnetic field emanating from a magnetized or electrified rail. The magnetic field perturbations are caused by material and structural variations within the rail, especially in the surface of the railhead. The entire thrust of magnetic rail inspection is to clearly distinguish between the magnetic field perturbations associated with critical flaws such as transverse fissures and those perturbations associated with extraneous noncritical flaws such as slight changes in metallurgical composition of the rail head. The three generic magnetic inspection techniques are residual magnetization, applied magnetization, and induced magnetization. Each of these generic inspection techniques utilizes a different aspect of the electrodynamic and/or magnetodynamic interaction of electric currents and/or magnetic fluxes with the rail structure. A brief review of each of these techniques is given herein.

3.1 Residual Magnetic Technique

In the residual magnetic (RM) technique a large magnetizing solenoid is moved along the railhead. This leaves a residual flux field longitudinally in the rail which gives rise to a leakage field in the immediate vicinity of rail flaws; this leakage field is then detected by search coils connected to a sensitive indicator. In the early years the RM technique was plagued with problems such as lack of sensitivity and poor discrimination. Renewed interest was sparked in it during the late 1930's when H. Keevil and coworkers of the Association of American Railroads (AAR) were finally able to make the RM technique practical using vacuum-tube amplifiers and more sensitive search coils.

In the years following, further improvements were incorporated using solid-state electronics and interlocking circuitry with a "no-burn" (NOB) coil searching under the railhead from the gage side, along with the addition of a smaller transverse magnetizer and sensor that was responsive to longitudinal defects like vertical split heads (VSH). Permanent records are now obtained for five channels across the railhead on a pen-chart recorder in the form of on-off indications. Several U.S. railroads today own, maintain, and operate AAR detector cars.

Two schemes are in use to reduce rail surface noise that can give false indications of flaws. The most common is the use of a small steel wheel rolling over the magnetized rail somewhat ahead of the pickup coils so as to "knock down" residual field perturbations caused by extraneous magnetic irregularities on the rail surface like filings and so forth. The advantage of this approach was discovered empirically and it is widely used. A similar result is obtained in another scheme whereby a relatively weak alternating magnetic field is superimposed on the residual field in the rail by a growler coil excited by low-frequency (800-Hz) alternating current prior to passage of the sensors over the surface. This latter scheme, however, is known to be in use on only one residual magnetic rail inspection car.

3.2 Applied Magnetic Technique

The applied magnetic (AM) technique relies on the application of a steady magnetic field to the rail, either along the rail (longitudinal) or across it (transverse). Any defects in the rail divert the magnetic field within as well as around the rail. Transverse defects affect a longitudinal field more than a transverse field, and similarly; longitudinal defects have their greatest influence on the transverse field. Defects divert the magnetic flux giving rise to perturbations in the magnetic field external to the rail which can be detected. However, with AM they must be sensed in the interpolar region. Longitudinal magnetization is preferred since the greater number and type of critical rail defects are transverse in nature.

The intuitive picture of the interaction of the applied magnetic field with the rail is greatly complicated when the applied field is moving relative to the rail, which is the typical situation in practical rail inspection. The nature of this velocity-dependent interaction is considered in Appendix B. Briefly, the pertinent results are as follows: The field-rail interaction is dominated by the quasi-magnetostatic flux-flow picture at inspection speeds considerably less than approximately 14 mi/hr. The quasi-magnetostatic picture is adequate in this region of operation. The velocity-dependent eddy-current generated magnetic effect dominates the field-rail interaction at inspection speeds considerably in excess of 14 mi/hr. The magnetostatic and eddy-current effects are comparable in a range of inspection speeds centered about 14 mi/hr.

3.3 Induction Magnetic Technique

The induction magnetic technique* is actually one where a large electric current (at low voltage) is passed throught the rail. The forerunner of the induction magnetic (IM) technique was a rail testing method pioneered by Dr. Sperry based on measuring variations in the voltage drop across a pair of closely spaced probes in contact with the rail carrying a large current. Whereas it worked satisfactorily in the laboratory, probe contact while moving was a problem in the field because of the variety of rail surface conditions; this prevented reliable results and led to many false indications. The voltage-drop method was finally abandoned in favor of replacing the probe contacts with several sensitive noncontacting search coils. These coils moved along the surface of the rail through which the large direct current is passing along at the same time. This large current creates a magnetic field around the rail which is perturbed by variations caused by internal fissures.

---

* This technique is also referred to as the direct-current-by-contact method.

As the search coils -- whose axes are at right angles to the rail --pass over the perturbed magnetic field, a signal related to the perturbed field is "sensed" by them. It is then amplified to transfer to a pen recorder a permanent record of flaw indications. The IM technique of rail inspection is offered by Sperry Rail Service (SRS) as a service to U.S. railroads and is available with an ultrasonic system supplementing the magnetic system.[3] Whereas an ultrasonic system "married with" the IM technique has been steadily improved since its introduction nearly twenty years ago, the basic IM method and configuration has remained unchanged.

3.4 Limitations to Overcome

There are inherent limitations in both the AAR RM and Sperry IM methods. Both have speed limitations imposed by the magnetic pole spacing in the RM case, and by the distance which is between the energizing current brushes in the IM case. The greater the spacing/distance ratio, the higher the inspection velocity can be. Another limitation has to do with workload of the operator who must continually monitor the pen chart records. At the same time, he must also visually observe track surface conditions and mark on the chart indications that cannot be attributed to transverse fissures or other dangerous (harmful) defects, i.e., those indications which can be associated with rail joint bars due to the large effect the bars have on leakage flux, as does the IM method especially at joints insulated for signaling purposes. It is mainly for the above reasons -- limitations in joint regions and operator workload -- that ultrasonic inspection techniques with their automatic processing have come into use over the past ten years or so.

Magnetic inspection cars of the AAR and Sperry types are capable of running at speeds up to about 15 mi/h (24 km/h), even with the need for simultaneous visual verification of some defect signals. However, occasional intermittent stops, or a rerun at a slower speed, are necessary to verify questionable defects under present operating procedures.

Such stops naturally reduce the amount of trackage that can be inspected during a normal day's work period. Hence, the usual distance covered is much less than the potential, i.e., inspection rates are more realistically 4 to 8 mi/h (6.5 to 13 km/h). At these operating speeds the sensitivity of the several magnetic pickup channels is set by the experienced detector car operator such that signals from nonharmful surface anomolies, i.e., especially engine burns, do not register too frequently so as to overload him, yet do appear as often as necessary to demonstrate adequate detection sensitivity to the various subsurface harmful defects that may be present. There is thus a definite, albeit intuitive and/or empirical, relationship between sensitivity and detection probability or confidence.

4. IMPROVEMENT OF EXISTING MAGNETIC TECHNIQUES

Several routes were followed in determining the extent to which it was necessary to address the various specific technical areas associated with advancing the state-of-the-art of magnetic rail testing. Contacts were made with many of the operating companies in the railroad industry which regularly use either their own residual mangetic detector cars or the rail testing service offered by Sperry with its line of induction magnetic cars. In addition, the Committee on Rail Testing and many knowledgeable experts on magnetic rail testing techniques, including many present and former detector car operators as well as some associated intimately with design and development of magnetic inspection cars, were solicited for their comments and assistance in this program. First-hand experience was gained by observing the practices involved in actual rail testing while riding with the crew on a hy-rail magnetic detector car on a major U.S. railroad. This broad exposure offered the opportunity of obtaining much useful information as to what courses to follow in attempting to advance the art of magnetic rail testing. Coupling this with a survey of the related literature on magnetic methods useful in nondestructive testing served to round out the knowledge gained.

A few pertinent facts became evident early in the formation of this program. The induction magnetic technique was eliminated from serious consideration as a rail testing technique worthy of study due to the fact that it is maintained, operated, and offered on a lease basis as a service to the railroads only by Sperry Rail Service. Thus it is treated as proprietary in nature by them, and in-depth information about the technical details of the system are not readily available. The applied magnetic technique has not knowingly been investigated and hence merits serious consideration. This technique has received considerable attention in the Soviet Union for many years, is well documented in technical literature, and appears to offer some advantages in overcoming certain limitations with respect to speed of testing. This technique has been investigated extensively from the theoretical/analytical point of view, but not nearly as much appears

regarding its experimental/practical use. Finally, the residual magnetic technique -- developed by the Association of American Railroads for the U.S. railroads -- emerged as a viable and trusted rail testing scheme that is rather widely accepted and used by many operating companies.

The technical details of the residual magnetic technique, however, have not been very thoroughly or widely documented. There appear to be several varieties of the basic AAR system in use today, with minor differences existing between the equipment configurations of individual users. This depends upon the nature of priorities set for the prevalent use of the car or the predominance of one or more types of defects to be sought out. In spite of the diversity existing in the RM technique equipment in the field, the types of records, and the actual testing policies employed, it was logical to draw upon this extensive source of information as a sort of reference starting point or "baseline".

Raw test data on track flaws detected by the residual magnetic method (AAR-type inspection cars) are essentially nonexistent. Voluminous records do exist in the form of strip chart records of up to six channels (per rail) for the various sensor coils. The pen-chart records are, however, step-function indications of the presence of track flaws after signal conditioning in comparator and combining (coincidence) circuits in the electronics of the system. As such, these signal records are unsuitable for analysis intended under the program. It was necessary to re-direct effort to set up full-scale experiments to obtain recordings of the actual raw signal responses to flaws of the various pickup coils integral to the residual magnetic inspection system in order to establish a baseline. Accordingly it was decided to emulate the flaw or defect signatures, i.e., the detailed amplitude-time histories, for several types of harmful (dangerous) defects and various surface anomalies (nonserious) that do occur in rail service.

4.1 Selection of Rail Defects and Anomalies

An aspect of rail inspection system testing that bears heavily on the credibility of the testing scheme is the fidelity of the sample flaws or defects which are employed. The nature of harmful rail defects, whether an ordinary transverse fissure or the less common compound fissure, is such that they are not easily duplicated artificially. This is readily understood when it is realized that natural rail defects occur usually after the rail has been in service for a long period of time and as a result of the continual wheel and axle loads imparted by the speed and type of train operation. The appearance (and growth) of a rail defect is also intimately related to the metallurgical history of the rail as well as the loads to which it is subjected. Similarly, factors such as temperature and weather changes can contribute to the cause of rail defects.

Rail flaws cannot be duplicated with sufficient fidelity, and the seasoned rail inspection specialist recognizes that there is no substitute for real defects. This is true whether they be of the harmful (dangerous) type, such as a detail fracture, or a surface anomaly like a nick or flaking, which are not serious defects but nontheless do frequently register as flaws on magnetic rail detection equipment. Thus, an important ingredient in this program is the availability of raw characteristic signal data from representative rail samples having actual defects, and these can only be obtained from an assemblage of known and characterized defects comprising a full-scale test track on which experiments can be run.

This need led to the defining of a set of experiments (low-speed) to be conducted on the Association of American Railroads' (AAR) 400-foot long test track at Chicago. Provisions were included not only for obtaining the needed raw data, but also for experimentally pursuing investigation of (a) techniques for improving rail magnetization, (b) new sensor designs, and (c) new magnetic techniques for rail inspection. The use of the AAR test track made it unnecessary to procure/fabricate track samples containing flaws of the type and variety necessary for conducting the program. The AAR test track has a mixture of jointed and

welded rail sections containing a broad cross section of well-documented natural dangerous and nonharmful defects. These include numerous transverse fissures up to at least 80 percent of the head area, compound fissures up to 40 percent, vertical and horizontal splits, several defective -- as well as good -- welds, some cuts, shelly spots, engine burns, and defects under burns*. Because of its relatively short length of 400 feet, however, this track was suitable only for low-speed use.

4.2 Means of Magnetizing the Rail

Various schemes have been used over the years to subject railroad rail to a magnetizing field while using magnetic sensing means to locate and identify rail flaws. Magnetic field sources customarily used are large electromagnets powered by a gasoline-engine driven d-c generator or other portable power sources. The ideal magnetizing circuit is one which has a magnetic core structure of infinite relative permeability and no air gaps or other nonmagnetic path lengths in the total magnetic circuit. To illustrate, consider a simple ring magnetic circuit. Suppose that the permeability of the ring core material is typically 1000, and assume that an air gap equal to 1 percent (1/100) of the ring mean magnetic path length were cut into the core. Under these assumptions the magnetic energy "lost" in the airgap, i.e., the magnetomotive force required to maintain the same flux in the air gap as the core, is nearly 90 percent of the total magnetic energy available. Or in other words, only 10 percent of the magnetomotive force is left to maintain the magnetic field in the whole remaining magnetic circuit. Similarly, if the net air gap length is less, say 0.25 percent (1/400), the magnetic energy lost to the airgap is still at least 70 percent. The latter assumed example is not unlike the situation that exists with a real magnetic structure associated with rail inspection. Practical reasons dictate that physical clearances on the order of 1/8-inch (3 mm) be maintained between the electromagnet structure and the head of the rail being inspected; this airgap is typical of that used in the AAR residual magnetism technique.

---

* Documentation for the test track used is contained in the Appendix A.

This program also involved the evaluation of new methods for magnetizing the rail, e.g., methods which presently are not used in the United States. These include two basic configurations for implementing the applied magnetic method as discussed previously, i.e., longitudinal and transverse magnetization. Longitudinal magnetization with a long inverted U-shaped magnet might also provide improved flux penetration for inspection at higher speeds. Magnetic flux sensors would be placed between the poles, i.e., within the active region of the magnet. Calculations indicate that increasing pole spacing to ∿10 ft will permit inspection speeds of approximately 25 mi/h (40 km/h) to be attained.

The ability to sense magnetic flux leakage changes while applying transverse magnetization to the rail may have certain advantages. It is hypothesized that eddy currents induced by the transverse field flow longitudinally along the rail head and return through the web and the base. Transverse defects can thus be detected by distortion of the current flow near the defect. Sensitivities comparable to those obtainable with the Sperry induction magnetic method might be provided without making electrical contact with the rail. Transverse magnetizaation may also provide improved inspection near the bolted joints.

Consideration was not given to methods of improving the induction magnetic technique due to the proprietary nature of that inspection service the consequent lack of technical information on design and performance. The program concerned, then, an investigation of the other magnetic techniques of rail inspection -- residual magnetic and applied magnetic -- as to magnetizing means in regard to aspects such as enhancing saturation, improving penetration of magnetic field, alleviating adverse speed effets, reducing equipment size/ weight and power requirements, as so forth. The conceptual approaches to this are shown in Figures 1 through 4 where the first illustrates the AAR (baseline) technique; the second, the high-speed applied magnetic (HSAM) technique; and the remaining, two versions of the low-speed applied magnetic technique for both longitudinal and transverse rail magnetization. The physical structure for guiding the detector

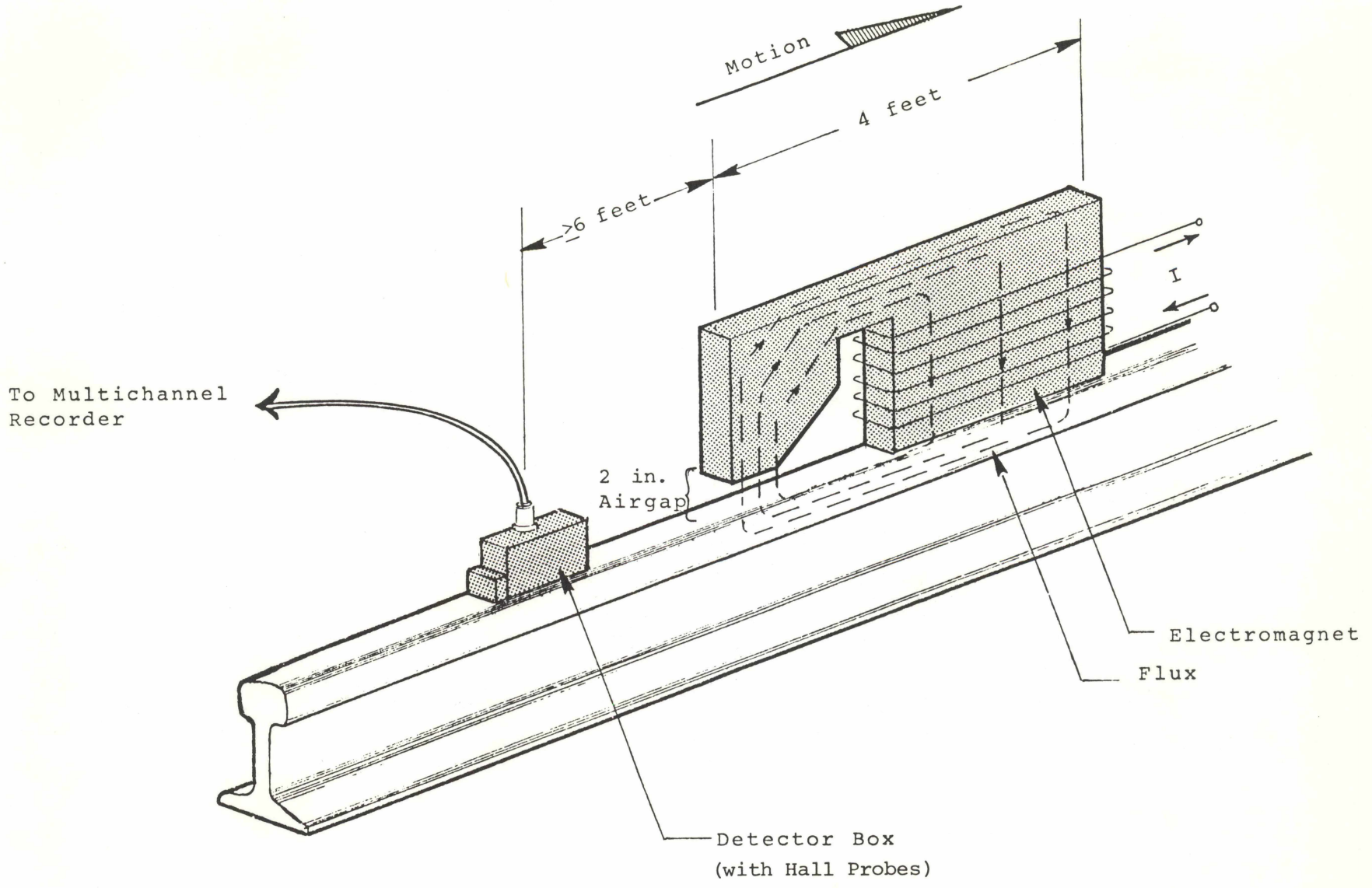

FIGURE 1. RESIDUAL MAGNETIC (AAR) METHOD

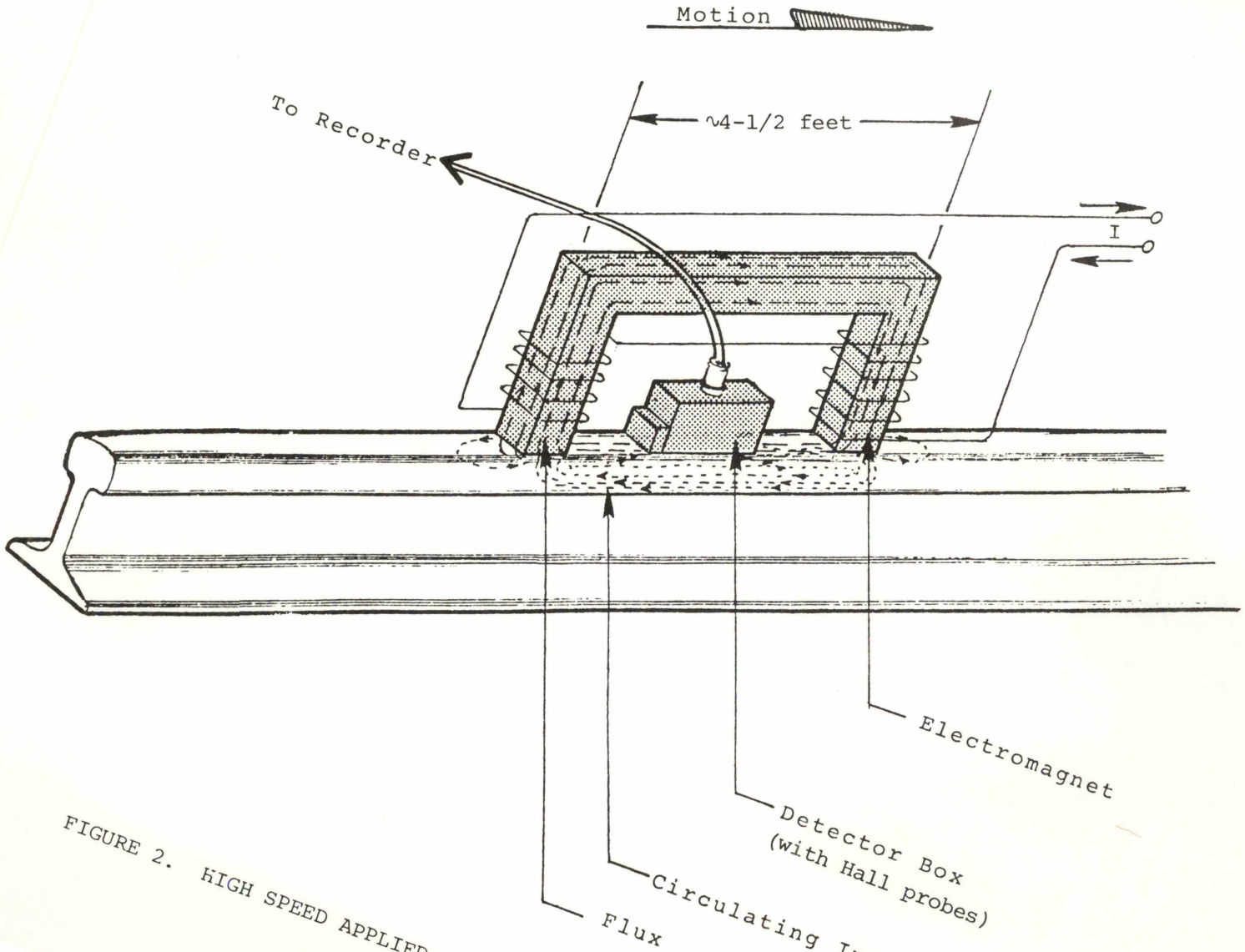

FIGURE 2. HIGH SPEED APPLIED MAGNETIC TECHNIQUE: EDDY CURRENT DOMINATED MODE

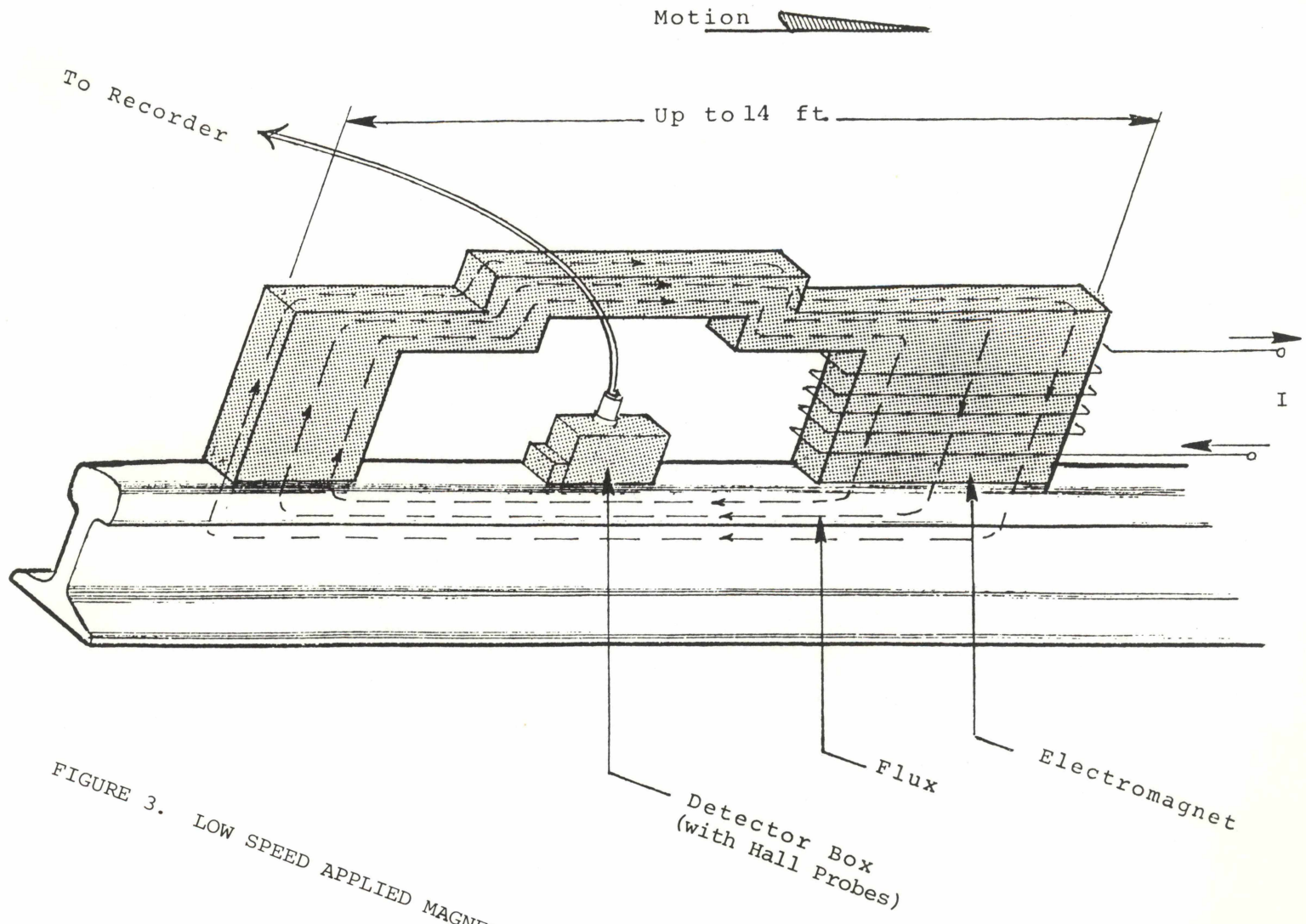

FIGURE 3. LOW SPEED APPLIED MAGNETIC TECHNIQUE: QUASI-MAGNETOSTATIC MODE

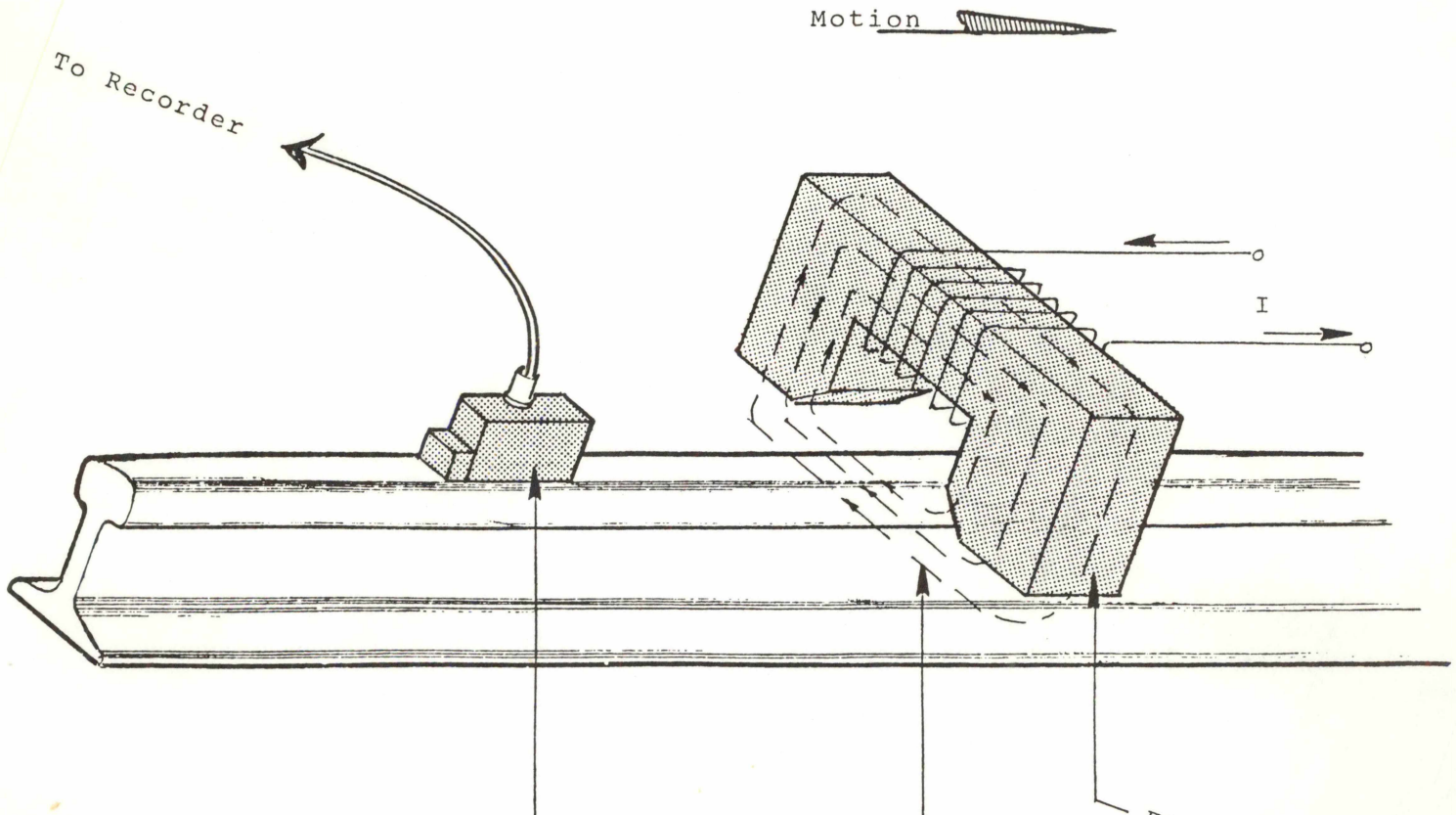

FIGURE 4. APPLIED MAGNETIC TECHNIQUE -- TRANSVERSE MAGNETIZATION

box carriage and other framework for supporting the magnet and poles have been omitted for the sake of clarity. The magnetizing structure and detector/sensor carriage was used on a single rail only, since provision had been made for only one set of apparatus. These four arrangements were chosen to utilize, insofar as practicable, various available standard AAR parts for the magnetizing circuit such as the coils, core pieces, top bars, supporting legs and wheels, and the detector carriage mentioned above. This approach has been taken to also minimize fabrication costs.

4.3 Magnetic Sensor Characteristics and Their Signals

If a ferromagnetic material is magnetized and it contains a near-surface imperfection, such as a crack or internal defect like a transverse fissure in rail, there will be a magnetic leakage flux in the vicinity of the material where the defect is located. The local magnetic field is greater in this vicinity than elsewhere around the material. If a device can sense either the external magnetic field (B_{ex}) or changes in it (dB_{ex}/dX) as it is moved over the surface containing the defect, the device will detect the higher local field and thus the defect. Assuming the device to be a search coil, a voltage will be induced across the coil terminals if the magnetic flux linking the coil changes. Cursory experiments show that the leakage flux around a body is a maximum when the material is at magnetic saturation, and it will remain substantially constant for the higher levels of applied magnetic field.[4] Follow-up experiments demonstrate that the leakage flux from a fatigue crack varies markedly depending on how "tight" it is; the leakage flux from much wider (sawed) slots varies much less with their widths.

A coil can be arranged in various physical ways as an induction pickup so as to have a preferred sensitive axis. Also, it can be made to respond proportionally to field strength or to the gradient (differentially) of the field in the case of dual coils on a common core. The coil responds only if there is a change in the flux linking it, i.e., if the field being sensed is changing strength with time or relative position. Thus, the coil is sensitive to the rate of change of magnetic flux with respect to time or motion.

Much attention has been given to the design of induction pickups having ferromagnetic cores. One of the principal parameters of the induction pickup is its sensitivity, i.e., the ratio of useful output to the strength of the field being measured. Very weak variable fields are capable of being measured. Induction pickups can be made either with an air core or with a ferromagnetic core to make them more compact. Adding a core makes the coil smaller and increases the sensitivity of the coil. Coil properties naturally depend on the design of the core as well as on the size and shape of the coil.

Procedures for selecting the core material and the major dimensions of the core to obtain maximum flux linkage have been worked out for the common core shapes. Cores for pickups are generally made of ferrite, Permalloy, or silicon-iron, and consideration must be given to the material properties since they depend on temperature, frequency, and level of the field or flux density. The higher the effective core permeability, the better the performance of the pickup. The optimum shape of a core is that which gives the maximum concentration of magnetic flux in the coil for a chosen stability. It should also be noted that as the core length-to-diameter ratio increases, the demagnetizing effects are reduced.

A different series of experiments[4] illustrates the effect of simple signal processing on the nature of the information content in search coil leakage flux signals. Without any signal processing, the signal amplitudes are proportional to defect depth (for a constant speed). However, in practical situations there usually is a low-frequency "noise" due to such items as a slight change in the sensor liftoff, but this can be removed by filtering or deliberately differentiating the search coil signal. It also has been demonstrated that the peaks of the differentiated signal are sharper than the corresponding leakage flux signals. However, there appears to be a limit to spatial resolution on the order of 0.040 inch (1 mm) unless exceptionally small sensors can be operated very close to the material. The ultimate useful sensor size has been claimed to be about 0.012 inch (0.3 mm), but the improvement over more practically sized sensors is questionable. But, smaller detectors do have a greater effect on increasing signal-to-noise ratio than on spatial resolution.

The Hall element, on the other hand, responds directly to the strength of a magnetic field rather than its derivative. In a few words, the Hall effect is the creation of a voltage across opposite edges of an electrical semiconductor when subjected to a magnetic field. The basis of this effect is the Lorenz force which depends on the deflection of charged particles (electrons) moving in an applied magnetic field. The force is mutally perpendicular to both the particle motion

and the magnetic field. Hall devices are made from both bulk materials and deposited thin films. They are available in a variety of shapes and sizes with active areas as small as 0.010 X 0.020 inch (0.25 X 0.50 mm) for high resolution to ten times that width and length for higher sensitivity. Magnetic fields ranging from 10^{-3} to 10^{5} gauss can be accommodated with appropriate electronics. Possible applications are virtually unlimited and include magnetic flux density measurement, gradient measurement, leakage flux mapping, residual magnetism determination, crack depth measurement, etc. An important advantage is lack of dependence on speed.

Another type of magnetic sensor is based on eddy current principles. If a metallic test object such as rail, is placed in the vicinity of an a-c magnetic field, eddy currents will be induced in the object. The eddy currents produce in turn an a-c magnetic field which can then be picked up by a coil or Hall element in close proximity to the object. The a-c magnetic field, thus sensed is "modified" by the test object's size, conductivity, and any inhomogeneities present such as cracks. If the object is ferromagnetic, its permeability also influences the a-c field effects, but saturating such an object in a strong dc magnetic field can nullify the effects of permeability. Depending upon the actual coil design -- be it probe, saddle, ferrite-cored, etc. --there usually is an optimum frequency which provides the best sensitivity to particular flaws. Often it is a matter of repeated experimentation to find the proper combination.

The eddy current method and the stray magnetic flux method have been compared for detecting surface cracks in rolled steel bars as well as for other flaw detection tests in tubes, bars, and billets.[5,6] Results from direct simultaneous comparison between the active (eddy current) and the passive (leakage flux) probes were displayed simultaneously. The experiments showed that eddy current probes are to be preferred for high resolution testing of smooth surfaces having flaws at or close to the surface. However, leakage flux techniques were found better for detecting subsurface flaws on materials with rough or very rough surfaces.

Differential magnetic stray flux probes offer better discrimination than a simple probe. Eddy current techniques were found quite unsuitable for testing rough surfaces[5], and leakage flux techniques were found able to resolve defect signals even with heavily scaled material. Further, reductions in noise levels of up to ten times have been obtained in practice by simultaneously exposing the test material to a combined constant field and alternating field magnetization, although a four-times noise suppression is more realistic.[6]

The coil, Hall element, and eddy current probe types of magnetic field sensors are all candidates for possible improvement of sensitivity and resolution in rail detection. Only the Hall element is insensitive to speed, however. Thus, improved sensor designs that appear most promising include Hall elements oriented to be responsive to three mutually perpendicular directions when placed immediately above the railhead. The pickup coils used were those of the AAR residual magnetism technique; these served as the baseline system, even though it is recognized that they are speed dependent. An array of Hall sensors and associated electronic instrumentation was used to measure the magnetic flux perturbations. Eddy current coils were also employed to detect surface anomalies or rail flaws such as cracks. A sketch of the array of Hall sensors and the eddy current coils employed for preliminary evaluation of the residual magnetic technique is shown in Figure 5.

4.4 Signal Processing Considerations

Signal processing techniques can be employed to find a flaw indicating method with greater sensitivity and reliability than obtained, for example, with the present AAR method. Review of analog strip chart records afford some idea as to what approach to follow. Joints have the most prominent signals, saturating the coil outputs in both positive and negative directions. Hall elements display a distinct "discriminator" curve, a gradually rising level that switches polarities abruptly and then gradually decreases. No other flaw produces these kinds of responses with such large magnitudes as do the rail joints.

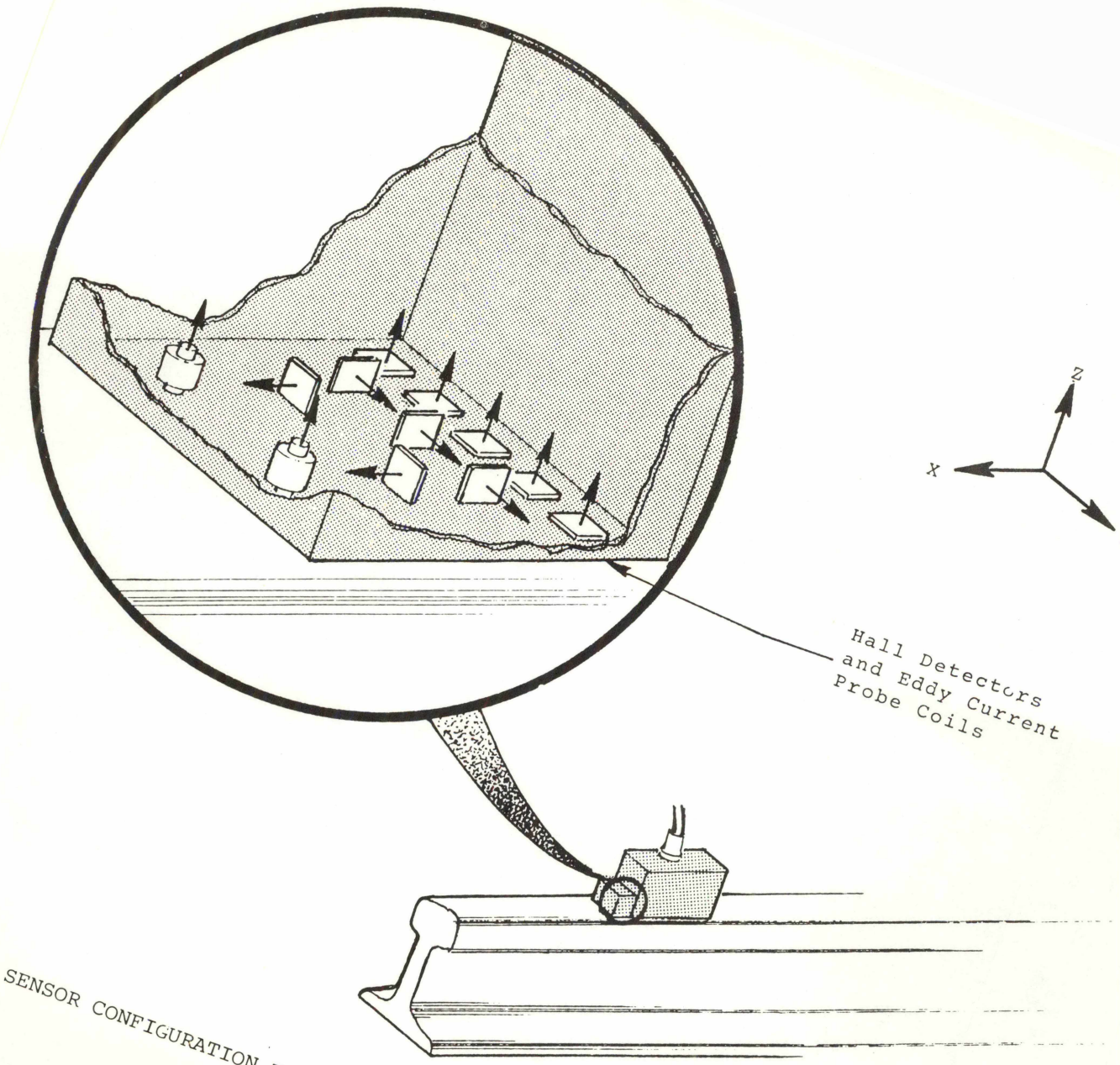

FIGURE 5. SENSOR CONFIGURATION TO BE USED IN INITIAL EXPERIMENTS

Flaw responses are fairly distinctive and have characteristic features. They usually possess fast rising edges and have a greater magnitude than the surrounding noise level. To find the flaws it is necessary to separate the flaw signal responses from the noise. Flaws can be more readily distinguished by enhancing the rate of change of the signal.

With these facts in mind, a digital computer can be used to process digitized raw data to develop flaw detection schemes. Special software is available to manipulate, display, and present the data. All of the analysis can be performed, for example, on a minicomputer with a graphics display terminal and an X-Y plotter added. Routines can be generated or are available so that signals can be differentiated, integrated, low- and high-pass filtered, modulated, thresholded (a base-band rejection technique), etc.

Before signal processing can begin, the data must be converted from analog to digital format. The conversion process samples the analog signal at a fixed interval and the magnitude of the signal is "quantized" by an anlog-to-digital convertor. To perform the actual sampling, a Digital Equipment Corporation PDP 11/40 minicomputer with a DEC laboratory peripheral system (LPS) was used. A conversion program causes the LPS to sample the signal and convert the magnitude to a signed 12-bit number at a fixed rate. This number is stored in the minicomputer's memory until enough data points have been gathered to fill a disk block, after which the accummulated data are read out. The process is continued until all the data are converted. In effect, this conversion process gives digital data points with an accuracy of about one millivolt over a range from ± 1 V. This is sufficient accuracy for any signal processing that follows.

The key concept governing such a digital sampling process is the Nyquist criterion. Briefly stated, to obtain a time representation of a continuous signal by using discrete points, it is necessary that the sampling rate be at least twice as great as the highest frequency component present in the original signal. If the input has components as high as 1000 Hz, then the signal must be sampled at a rate not less than 2000 times a second. Now suppose the sampling rate is below this

"Nyquist frequency"; say the rate is still 2000 times a second, but there are signal components as high as 10,000 Hz. Low-frequency components will be counted in with the higher frequency components, giving an amplitude that is greater than that truly present and distorting the discrete signal. This effect is known as "aliasing" and can be avoided if the continuous signal is low-pass filtered, with a cutoff frequency set at or below the desired sampling rate, before it passes into the converter.

From these considerations, the first step in designing the conversion system is to determine the maximum frequency which is contained in the useful (or non-noise) signal. This appears to be about 120 hz for a speed of 4 mi/h (6.5 km/h) especially for the spiked flawlike responses. Second, the maximum frequency is known only approximately by studies on a spectrum analyzer. To provide a margin for some error, the sampling rate used was 600 Hz; to avoid aliasing, a four-pole low-pass Butterworth filter with a cutoff at 500 Hz limited the signal spectra.

A graphics display routine can be used to "reconstruct" and "process" the signal data as desired. To use the routine the analyst begins with the short section of the record that appears on the graphics display and selects any of the various processing methods that can be applied to the signal. After processing, the results on the display can be copied by using the plotter.

Enhancement of the edges of flaw signals can be accomplished by differentiation. By then using the threshold capability, only those spikes with edges steeper than the threshold minimum show up. Most of the noise is thus removed, yet, if the threshold level is set too low or a noise spike is sufficiently sharp, false indications may appear.

4.5 Rail Defect Signals

The nature and characteristics of rail defect signals picked up by magnetic sensors are not unlike those found by other leakage flux test methods. Some comments regarding the general nature of those appeared previously in the section of this report titled Magnetic Sensor Characteristics and Their Signals. Very little raw data, however, existed prior to this program for actual rail defect signals from AAR pickup coils. What were available are in the form of film strips which were made by exposing a 35-mm film moving across the face of an oscilloscope which had a coil output signal connected to its vertical input. It was quite enlightening to be able to obtain the variety of signals encountered in this program and subsequently analyze them.

These signals fall roughly into two categories, the "discriminator" and the "schmoo" curves; Figure 6 shows both of the curves. As mentioned earlier, the discriminator curve has a rising edge followed by a polarity change and then a dropping edge that eventually returns to the ambient level. A schmoo curve, on the other hand, has a short fast rising edge followed by a rapidly falling sweep that always goes negative, rises again to a positive level, and then falls back to the noise level. The schmoo resembles the letter M with the center leg carried below the other two legs.

Abrupt cracks in rail transverse to the direction of the magnetic field generate a schmoo curve when sensed by a coil. Hence, flaws like detail fractures and transverse fissures, as well as rail joints and welds, are identified by the schmoo curve. A joint produces, in general, a much stronger response than a transverse fissure and this allows for easy separation of these two. The same kind of flaw produces a discriminator curve when sensed by a Hall element. The difference between the two sensor outputs is that the Hall element responds to changes in the magnetic field, while the coil responds to changes in the derivative of the magnetic field. Hence the schmoo curve is the derivative of the discriminator curve.

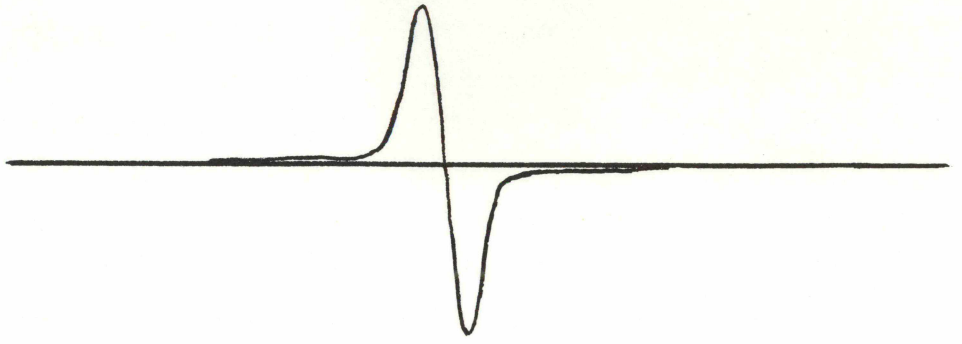

(a) Discriminator

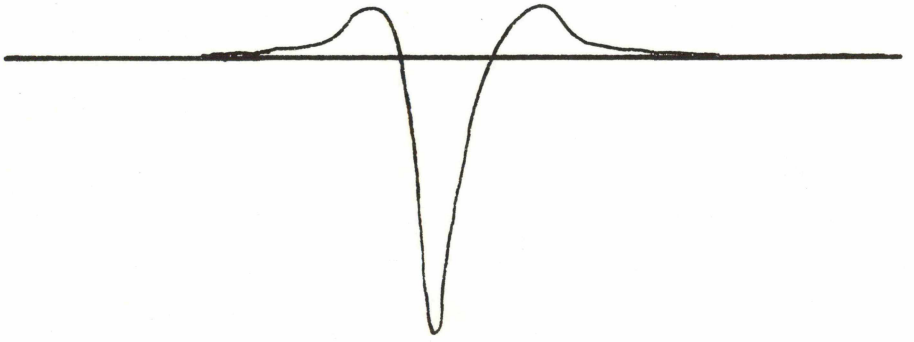

(b) Schmoo

FIGURE 6. REPRESENTATIVE ANALOG SIGNAL RESPONSES OF TRANSVERSE DEFECTS

Compound fissures sometimes respond like transverse fissures and produce a strong schmoo signal, but at other times they generate a discriminator response. This apparent anomaly is due to the precise nature of the defect. If the compound fissure has very pronounced vertical cracks and a relatively minor horizontal crack, a schmoo curve should be seen. If the fissure has a greater horizontal then vertical component, then the discriminator curve results.

Vertical split heads do not give a clearly characteristic signal and are thus difficult to identify. Similarly, engine burns are also difficult to detect by magnetic testing, but are relatively easy to identify visually. If an engine burn has a fracture associated with it underneath, it indeed will be easily detected magnetically.

As a further enhancement, a system of voting circuits much like the AAR interlocking network can be used, especially if low-level flaw responses are to be found among the noise. A voting circuit will only generate an output if a signal appears at the same time on two or more different sensor channels. Sudden changes caused by noise may generate flawlike indications in a sensor, but if the noise is contained within a single channel only the voting circuit will recognize the signal as a flaw if other channels have a similar response at the same time.

In addition to detecting flaws, it is highly desirable to automatically classify and/or measure the size of flaws. The total system would then need little operator intervention, thus relieving the operator of this burden. The extent to which flaws can be classified automatically depends on how distinctive the sensor signals generated by each type of flaw are relative to each other. To do this requires a pattern-recognition system, and even a cursory examination indicates that no simple analog method is available to classify the flaws. A digital approach will be necessary, but in order to be sucessful quite extensive information must be obtained about each and every type of possible flaw.

For the time being, then, the rail flaw indicating system can be conceptually viewed as in Figure 7.

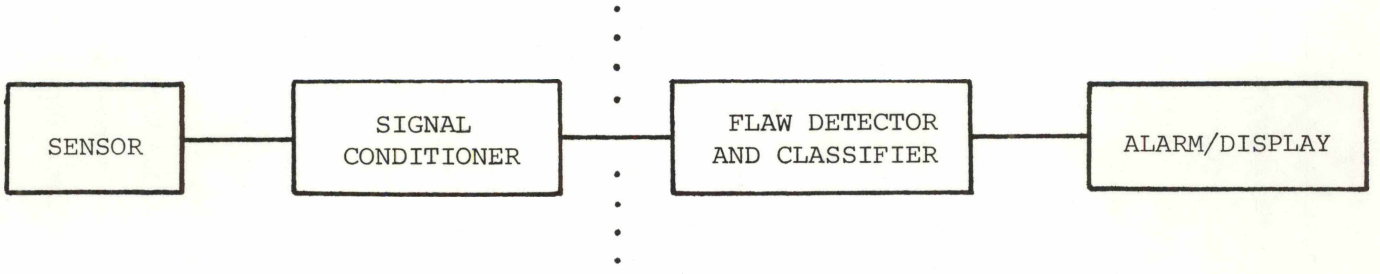

FIGURE 7. A CONCEPT FOR RAIL FLAW DETECTION AND CLASSIFICATION

5. INVESTIGATION OF NEW MAGNETIC TECHNIQUES

Early review of magnetic inspection techniques applicable to rail indicated that two different approaches to supplying the magnetic field merited further investigation. These two were the low-speed applied magnetic (LSAM) technique and the high-speed applied magnetic technique (HSAM). As noted previously, the AM technique relies on the sensing within an applied moving active magnetic field the perturbations in that field above the surface of a rail in which flaws are present. Magnetization along the rail direction enhances the detection and location of the more harmful defects such as transverse fissures.

The HSAM technique induces circulating (eddy) currents in the upper part of the railhead by means of a moving magnetic field. When these circulating currents are intercepted (interrupted) by transverse defects, magnetic field perturbations can be picked up by sensors located between the poles. Increasing speed increases the magnitude of induced currents but will limit depth of penetration. In addition, a greater signal is generated in the search coils at the higher speeds because of the more rapid rate of flux change in the flaw region. Calculations also indicate that small (<10% area) transverse defects can go undetected by this method, depending on how deep they lie beneath the surface of the rail. The ability to detect gross defects at high speeds, i.e., greater than 25 mi/h (40 km/h) is claimed by the Soviet investigators.

A variation on the HSAM technique is to consider transverse magnetization instead of longitudinal magnetization, so as to cause circulating currents to occur mainly in the vertical plane (web) of the rail. These currents, too, have longitudinal components that are intercepted by transverse defects and the field perturbations detected. Here as speed increases, though, the currents move away from the central area of the railhead and out to the edges. While this might be better for detection of detail fractures from shelling, it would reduce center-head coverage.

An electromagnet and detector carriage assembly were employed to evaluate some of the techniques for improvement. These include the Hall devices which replaced the standard pickup coils which sense the magnetic field and eddy current sensors which were used to measure surface defects such as engine burns. Various magnetizing pole configurations having potential for increasing the maximum speed of test car operation were also evaluated with the carriage assembly. An out-of-service AAR-type inspection car was considered for use as a test carriage. However, it could not be readily adapted to accommodate the special structures to be investigated, i.e., such as that for the applied magnetic method which required magnet pole separations greater than 10 ft. A TSC-supplied heavy-duty aluminum car, the Safetran Model 500, was also considered for carrying the carriage, instrumentation, and power sources. However, it also proved not feasible as a means of supporting the carriage assembly and the heavy and bulky mangetizing structures planned.

The arrangement for the apparatus as eventually constructed consisted of two rigidly coupled carts 14-ft long (overall). This afforded a total of four magnetic inspection schemes with a variety of magnetic sensor options. The carts were assembled from structural aluminum channel welded and/or bolted to 1/2-inch thick plates plus angle stock. These two rigid boxlike frames served as the support for the several types of magnetizing structures and sensor carriage options and locations. The two (fore and aft) cars were joined by rigid members and pulled by a hy-rail vehicle. As assembled the test apparatus was configured to duplicate the AAR residual magnetic method of rail inspection for right-hand running only. It was also readily modifiable to simulate both the longitudinal and transverse applied magnetic methods. Readily available AAR rail detector car parts were leased through R.D.C. Parts Company, Inc., thus making it unnecessary to fabricate numerous specialized items. The leased items included the Model 8 magnet, wheel supports, complete pickup carriage assembly, and pickup boxes (main, NOB, and VSH). The general configurations of the test apparatus used in full-scale experiments on the AAR test track are sketched in Figures 8 through 11.

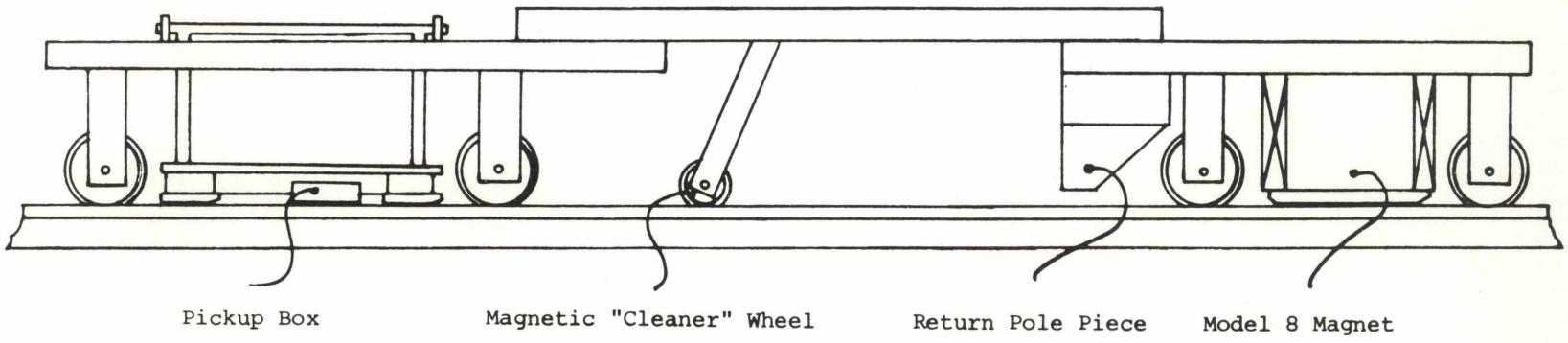

FIGURE 8. RESIDUAL MAGNETIC TECHNIQUE

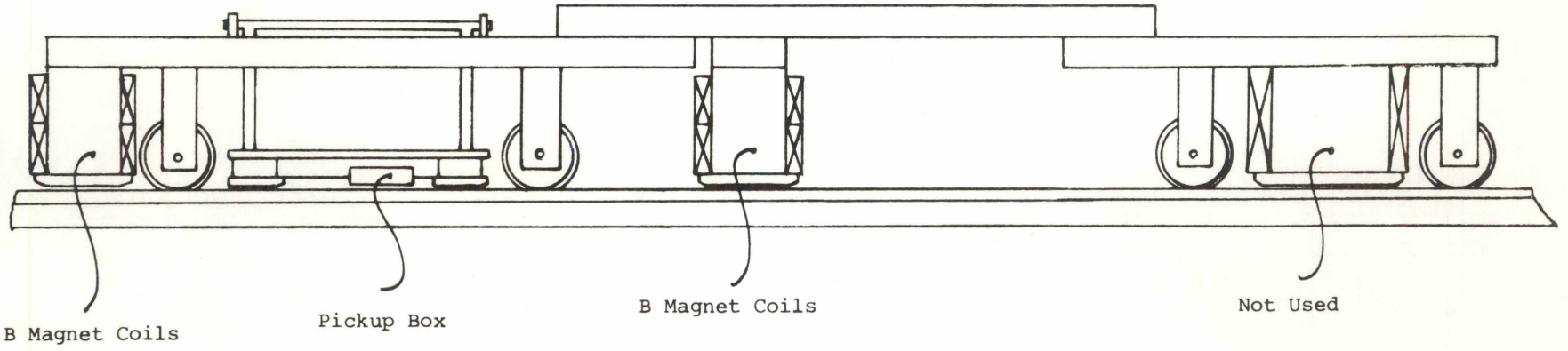

FIGURE 9. HSAM TECHNIQUE - LONGITUDINAL MAGNETIZATION
(Carriage support mechanism is not shown.)

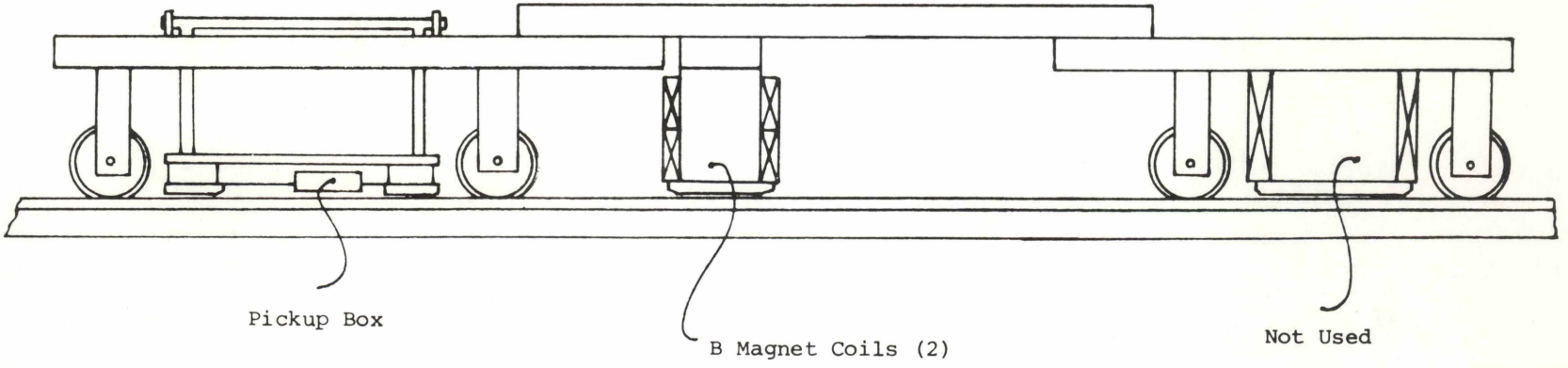

FIGURE 10. APPLIED MAGNETIC TECHNIQUE -- TRANSVERSE MAGNETIZATION
(Carriage support mechanism is not shown.)

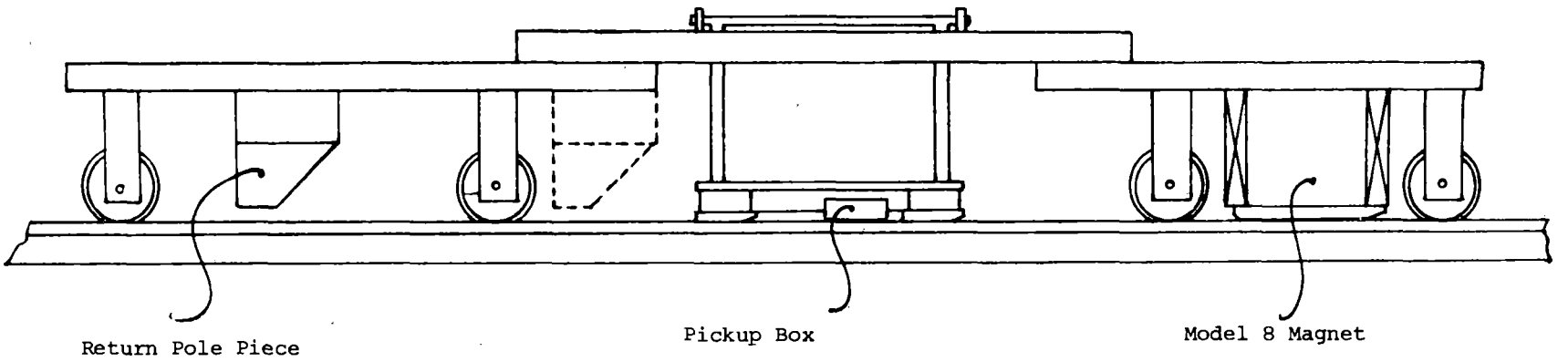

FIGURE 11. LSAM TECHNIQUE -- LONGITUDINAL MAGNETIZATION
(Carriage support mechanism is not shown.)

The standard 5-3/4-inch long AAR pickup box was used as a benchmark to compare with other sensors such as Hall elements and eddy current probe coils. This pickup box contains five differentially wound coils physically arranged to give coverage of (a) the gage corner, (b) top of rail near gage side, (c) middle top of rail (broad coverage), (d) top of rail favoring field side, and (e) top of rail favoring gage side. A sixth sensor, the NOB (no-burn) pickup coil, rides against the gage side of the rail and "looks" horizontally toward rail center under any top rail surface anomalies. This coverage is sketched in Figure 12. Several coils are interlocked in the AAR detection scheme to offer detection decision logic that aids the operator in determining more precisely the nature of rail flaws indicated on the pen chart readout. For example, the NOB coil is interlocked with the gage corner coil so as to get a combined channel indication when a flaw is not an engine burn, but rather a defect such as a fracture under a burn or a welded burn fracture. The coil for top of rail near gage side is interlocked with both the center-coverage coil and the NOB coil, again to assist the operator in sorting out surface anomalies such as engine burns from harmful defects.

Hall elements* were installed in a linear array fashion in a 1-inch square lucite block. Five of the elements were spaced on 3/8-inch centers in the block to span the rail head (over a 2-inch width starting from the gage side), being sensitive to the components of magnetic flux normal to one of the 3-inch long edges. In this way the line of these five elements was transverse to the rail and it could be arranged either vertically or horizontally to "sweep" the railhead and be responsive to the component of leakage flux respectively either longitudinal with the rail or normal/vertical to its top surface. A second group of two Hall elements was located in the same 1-inch square lucite block immediately behind the line of the other five so as to be responsive to the component of leakage flux horizontal but transverse to

---

* F. W. Bell Model BH-700 high-sensitivity transverse type.

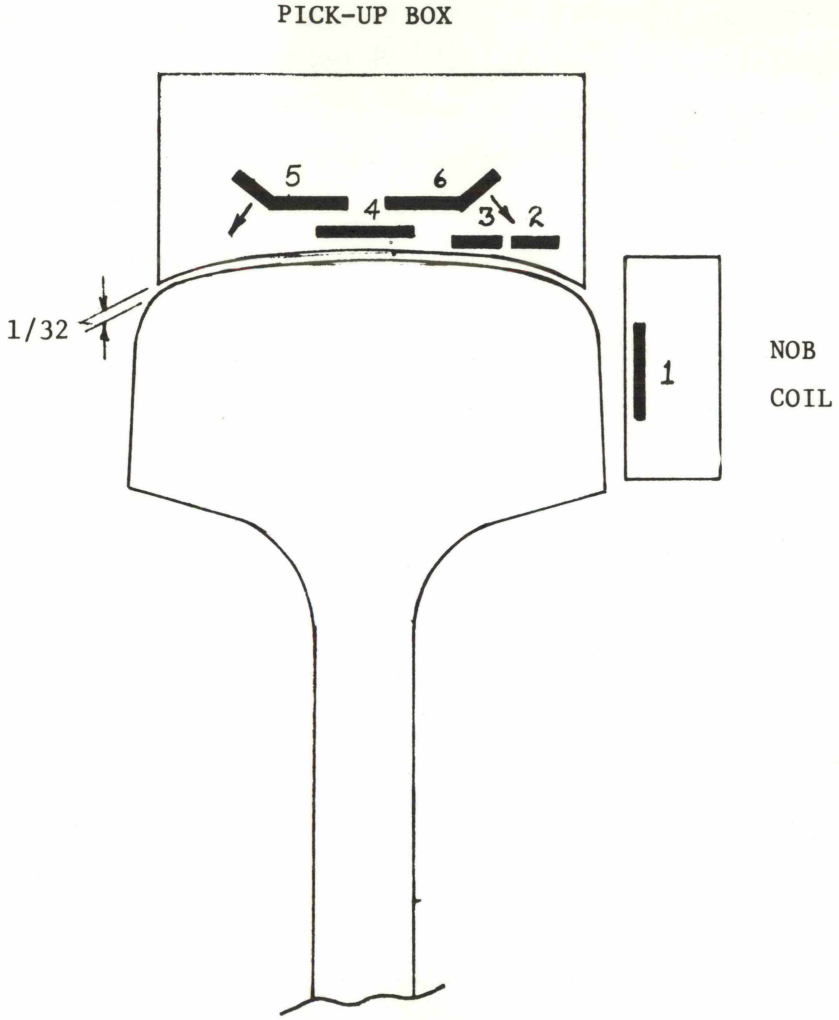

FIGURE 12. SKETCH OF AAR PICKUP COILS

the rail. With these two groups of Hall elements, it is possible to simultaneously monitor two of the three orthogonal leakage flux components in the two perpendicular positions, thereby obtaining information on all three orthogonal components. (Contrast this to the coil-core type of magnetic sensors in the main AAR pickup box which are oriented to be responsive only to the change in the vertical plane components along the direction of motion; only one coil-core sensor -- the VSH pickup -- is configured to favor a transverse component of magnetic field.)

Another group of three Hall elements was arranged in a second lucite block attached to the first with a nylon screw and hanging down along the gage side of the railhead in the space where the normal wheel flange passes. This side block could thus pivot out of the way if it came in contact with an obstruction along the rail in the flangeway space. The three Hall elements in this side block were oriented to be responsive to both the transverse and longitudinal leakage flux components along the gage side of the rail, much like the NOB (no-burn) pickup is in the AAR magnetic inspection system. Thus, a total of nine Hall elements was available to simultaneously monitor rail leakage flux. The layout of these is shown in Figure 13.

All the Hall elements were originally wired in series to have the same control current (0.2 ampere across $\sim$4 ohms) and allow for a single control supply. The Hall voltage output from each element was amplified by individual balanced single-stage solid-state preamplifiers having typically a gain of 50X and provisions for nulling the offset voltage. Since the Hall voltage at the element terminals was anticipated to be only a fraction of a millivolt for the stated product sensitivity, some amplification was deemed necessary. Upon check out of the Hall sensor assembly, it was found that the individual elements could not share a common control current supply because of the "ladder effect" which precluded nulling of the offset voltages for all but the two elements in the center of the string. Hence, it became necessary to "unbundle" the control current leads and provide a separate current source for each element. After this was done it was possible to null out each element separately.

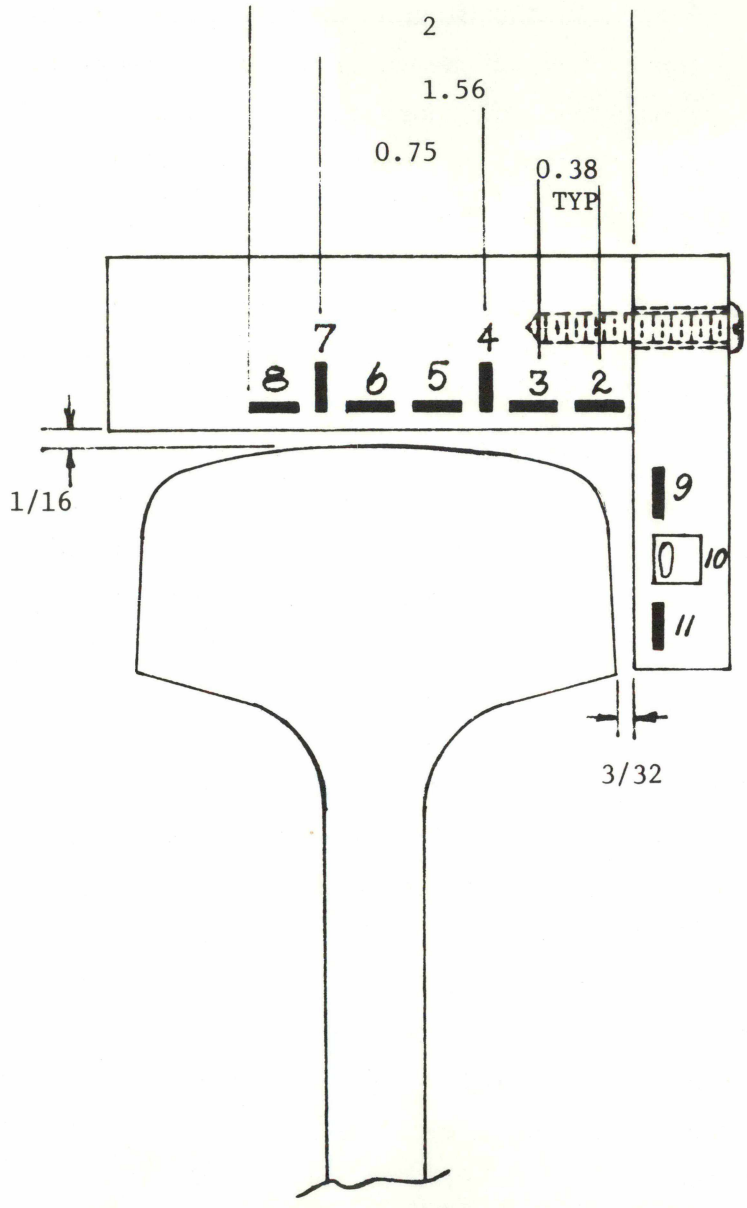

FIGURE 13. LAYOUT OF HALL ELEMENT SENSORS

Laboratory experimentation with eddy current inspection techniques on a cold-rolled steel block led to the selection of a 1/4-inch ferrite-core probe coil with operation at 920 Hz. The test block had a rectangular cross section similar to the conventional railhead and a selection of narrow (∿0.025 inch) machined slots, both transverse (various depths) and longitudinal (edge and center locations), to simulate rail flaws. A Nortec NDT-15 Eddyscope was tried with a variety of available test coils at various frequencies for each. The NDT-15 offered the advantages of a wide frequency range (100 Hz to 4 MHz), high gain, automatic nulling, simultaneous phase/amplitude display on a self-contained storage oscilloscope, and high sensitivity. Flaw indications were found to be sensitive not only to liftoff, characteristic of eddy current inspection, but also to the permeability of the steel test block besides the conductivity changes due to each slot. (In eddy current inspection of ferromagnetic materials, the material may be magnetically saturated to reduce spurious signals caused by permeability changes not associated with the presence of flaws.)

6. EXPERIMENTS CONDUCTED WITH RAIL FLAW DETECTION SCHEMES

6.1 Preparation and Operation of Test Apparatus

A "universal" test apparatus was designed and constructed to allow implementing the various magnetizing and sensor arrangements described in preceeding sections. To begin with, the test carts, magnetizing structures, portable generator, carriage assembly (without pickup box installed), and interconnecting rigid channel members were assembled at the AAR test site. Some reworking of the front cart was necessary to position the Model 8 AAR-type magnet symmetrically over the railhead because the anticipated clearance between the magnet coil and cart side frame was insufficient. Nonetheless, after assembly the test apparatus was given a general shakedown on the test track at speeds up to nearly 20 mi/h. It was necessary after this shakedown to retighten several frame bolts, put additional bolts in some members, and regage the axle shafts for some of the flanged wheels on the carts. The test apparatus rode rather "hard" since it was a rigid assembly; otherwise, the performance was satisfactory.

After shakedown, the instrumentation was added by completing assembly of the carriage and pickup box (with NOB coil) on the rear cart. An Ectron multichannel instrumentation preamplifier, a Sangamo SABRE VI FM tape recorder, 16-channel active filter box, and Honeywell Model 1858 Visicorder light-beam oscillograph were installed in the back-seat area of the IH Wagoneer hy-rail towing vehicle. This resulted in signal cable lengths of about 25 ft between the sensors and the instrumentation. This was necessary because shock forces imparted to the carts while running made it unwise to place sensitive instrumentation on the carts. Of necessity, the boxed set of ten Hall element preamplifiers and power supplies, and the eddyscope, had to be mounted near (<3 ft) the main AAR coil pickup box where their sensors were placed, but these were

suitably shock-isolated with flexible 4-inch thick foam pads and "soft" tie-downs. The Hall element array was affixed to the rear surface of the pickup box with a combination of double-backed bonding tape and glass-fiber reinforced strapping tape. A 1/2-inch-square by 2-3/4-inch long bakelite block was used to space the Hall array away from the stainless steel pickup box. The planar array of five Hall elements was set in either a vertical or horizontal plane, as desired. When the eddy current probe was used, it was similarly mounted to the rear gage runner riser on the carriage assembly with a track clearance of about 3/32-inch.

The instrumentation was first operated from building power (115 V ac) to checkout the setup. The Hall elements and preamplifiers were battery powered. Upon energizing the magnet with the instrumentation operating, it was found that the static (dc) component of flux sensed by the Hall elements was overloading the instrumentation. In addition, strong interaction between/among the various Hall output voltages from the preamplifiers occurred and upset the null (zero) adjustments of the light-beam oscillograph and FM tape recorder. Corrective action taken to eliminate these difficulties consisted of (a) inserting high-pass filters (a 25-μF series nonpolarized capacitor and a 470-ohm shunt resistor) at the output of each Hall preamplifier, and (b) removing a "common" tie point (grounding) among all the Hall output signals. It was necessary also to insure that all signal "grounds" were individually isolated from one another as well as from any other metallic surfaces such as the hy-rail body/chassis or the frames of the carts; this minimized ground-loop current problems.

Another source of difficulty arose when the instrumentation in the hy-rail was powered from the portable generator on the cart as required to operate on the test track. The gasoline-engine driven generator was a source of vibration to the front cart. Signal cabling was found to be sensitive to this vibration; however, this was reduced by suspending it away from the carts, drawbar link, and towing vehicle. The generator speed -- 3600 rpm -- was also discovered to be a source of 60-Hz "hash" noise in the instrumentation.

These extraneous signals were quite troublesome and required a radical change in the cabling between the instrumentation preamplifier inputs and the various sensors, i.e., pickup coil or Hall element signals. Two-conductor balanced cables, (shielded and jacketed) were substituted for all coaxial unbalanced cables initially used to connect the pickup box (coils) and preamplified Hall signals to the instrumentation preamplifier. The shield could be grounded only at the inputs to the instrumentation pre-amplifier. A common ground tie point between all five coils in the AAR main pickup box existed internally and could not be changed.

Other means were also used to improve the signal-to-noise ratio. The most successful scheme consisted of one used in public address systems where the impedance at the distant end of a long cable run is made a low impedance, like 100 ohms, to reduce hum pickup. Since all coil resistances are typically thousands of ohms, and the instrumentation preamplifier input resistances are 50 K to 100 K ohms., the signal-to-noise ratio was considerably improved by shunting each line with a 3.9-ohm resistor and increasing the gain to compensate. (The 470-ohm resistors in the Hall signal output lines could not be so shunted without suffering from insufficient gain; thus this allowed a somewhat higher noise level.)

Two gasoline-engine driven ac generators were used. One supplied rectified and filtered direct current to energize the magnets and the other was used for the instrumentation. Experiments were run for four different test configurations, as follows:

A - residual magnetic AAR technique

B - high speed applied magnetic technique, longitudinal magnetization

C - low speed applied magnetic technique, transverse magnetization

D - low speed applied magnetic technique, longitudinal magnetization.

Figures 14 and 15 show two views of the test carts, the magnetizing structures, and pickup carriage assembly arranged for Configuration A (AAR) tests, the instrumentation, and the hy-rail vehicle used. (These four apparatus configurations were described in detail earlier and illustrated previously in Figures 8 through 11.

A total of 30 experimental runs for these four test configurations were made during a three-day period with various sensor arrangements. Up to 12 data channels, plus an event marker operated once per wheel revolution, were recorded. The AAR-type main pickup box with NOB coil was used for all configurations, except where the VSH pickup coil replaced it for a few runs of Configuration C. The NOB coil and coils #2 and #4 served as common sensors for all runs (except when the VSH coil was used). Test speeds were approximately 4 mi/h for all configurations, and for Configuration D runs were made at 4, 10, and 15 mi/h. At the highest speed (15 mi/h) the carriage assembly bounced considerably, with the result that the sensor output signals were affected by this vibrational motion. A summary of the several test runs and the associated configurations and sensor options used appears in Table 1. Figures 14 through 18 show some views of the various apparatus arrangements. A close-up view of the complete detector carriage assembly is shown in Figure 19 from the gage side of the track.

TABLE 1. TEST RUNS ON AAR TEST TRACK

Run No.	Configuration[a]	Data Channel/Sensor[b] 1	2	3	4	5	6	7	8	9	10	11	12	Notes
4-1	A	NOB	C#2	C#3	C#4	C#5	C#6	HE2	HE3	HE4	HE5	HE6	HE7	4 mi/h (to Run 6-6)
4-2														
4-3														
4-4				HE9		HE8	HE11							
4-5														
4-6														All gains low
4-7	B													
4-8				C#3		C#5	C#6							
4-9														
4-10														All gains high
5-1								(c)	(c)		(c)	(c)		
5-2				HE9		HE8[c]	HE11	(c)	(c)		(c)	(c)		
5-3	A					(c)		(c)	(c)		(c)	(c)		Without magnetic cleaner wheel
5-4						(c)		(c)	(c)		(c)	(c)		Magnet not energized
5-5						(c)		(c)	(c)		(c)	(c)		
5-6						(c)		(c)	(c)		(c)	(c)		
5-7	C					(c)	--	(c)	(c)		(c)	(c)		HE11 went defective
5-8						(c)	--	(c)	(c)		(c)	(c)		
5-9						(c)	--	(c)	(c)		(c)	(c)		
5-10		VSH[d]	--	--	--	--	--	--	--	--	--	--	--	
5-11			--	HE9	--	HE8[c]	--	HE2[c]	HE3[c]	HE4	HE5[c]	HE6[c]	HE7	
5-12			--		--	(c)	--	(c)	(c)		(c)	(c)		
6-1	D-6	NOB	C#2		C#4	EC(H)	EC(V)	HE2	HE3		HE5	HE6		
6-2														HE7 noisey
6-3														HE7 okay
6-4	D-11.5													
6-5													--	HE7 turned off
6-6													--	10 mi/h
6-7													--	15 mi/h
6-8													--	15 mi/h

(a) A - residual magnetic (AAR) technique; Figure 8.
B - HSAM technique; Figure 9.
C - transverse applied magnetic field; Figure 10.
D-6 - LSAM, 6-ft pole spacing; Figure 11.
D-11.5 - LSAM, 11.5-ft pole spacing; Figure 11.

(b) NOB - no-burn coil, No. 1
VSH - vertical split head coil
C#2 - coil No. 2; etc.
HE2 - Hall element NO. 2; etc.
E(H) - Eddy current probe; horizontal (lifeoff) channel
E(V) - Eddy current probe; vertical (signal) channel

(c) Hall element Nos. 2, 3, 5, 6, and 8 are in vertical transverse plane, otherwise, these sensors are in horizontal plane (transverse alignment).

(d) VSH coil replaced NOB/main pickup box.

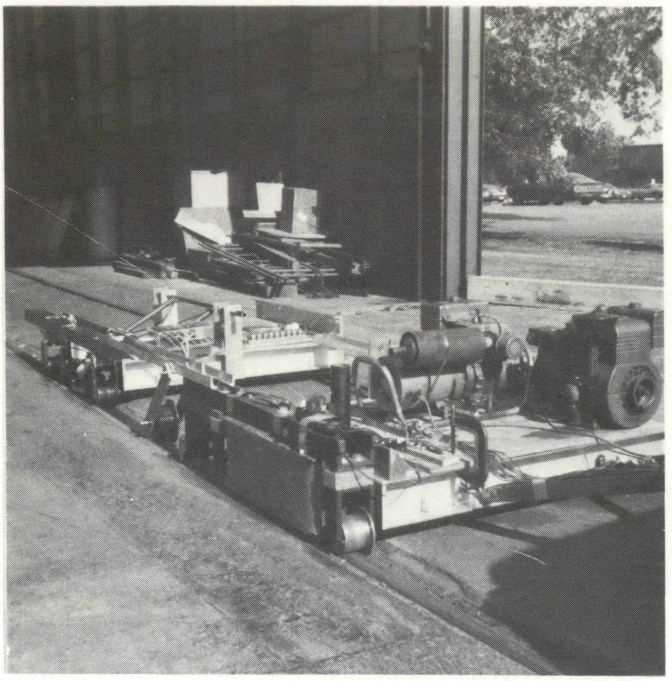

FIGURE 14. FRONT VIEW OF RAIL TESTING APPARATUS SET UP FOR CONFIGURATION A

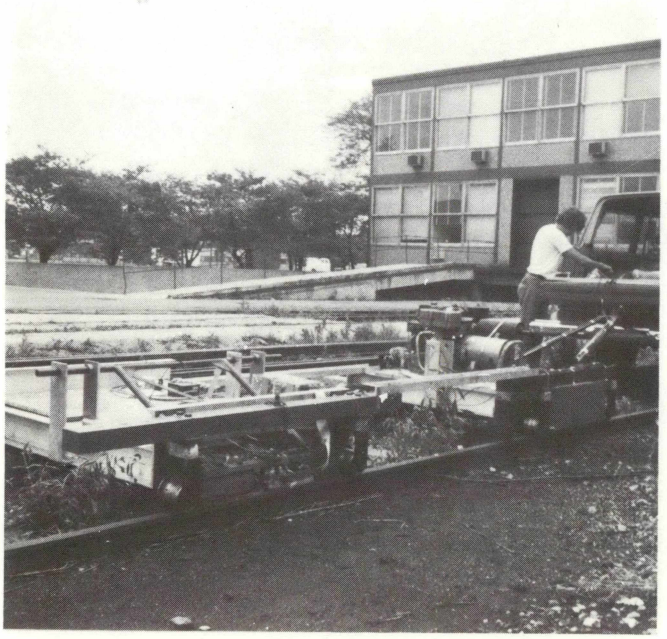

FIGURE 15. REAR VIEW OF CONFIGURATION A TESTING APPARATUS AND TOWING HY-RAIL VEHICLE ON TEST TRACK

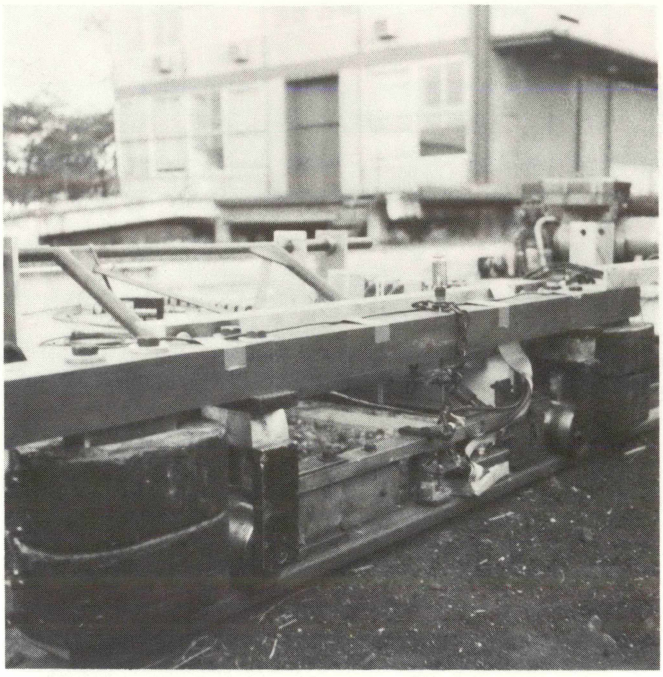

FIGURE 16. VIEW OF REAR CART SET UP FOR CONFIGURATION B

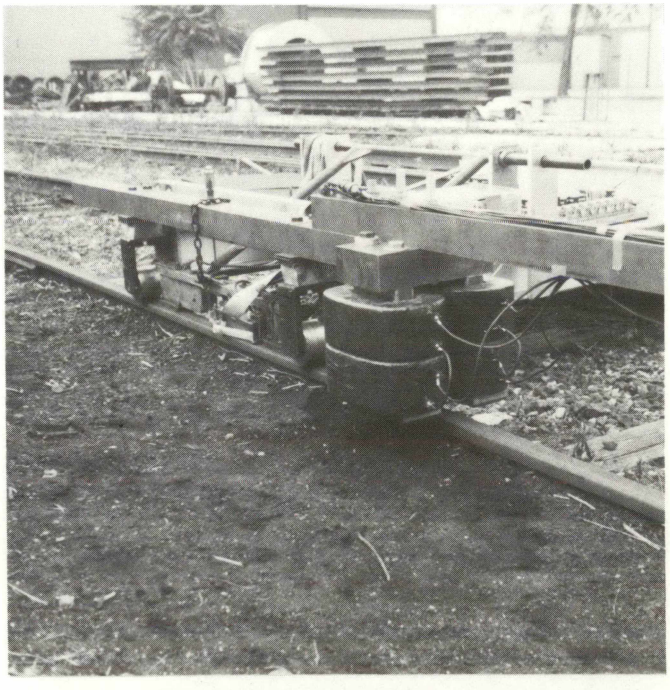

FIGURE 17. VIEW OF REAR CART SET UP FOR CONFIGURATION C

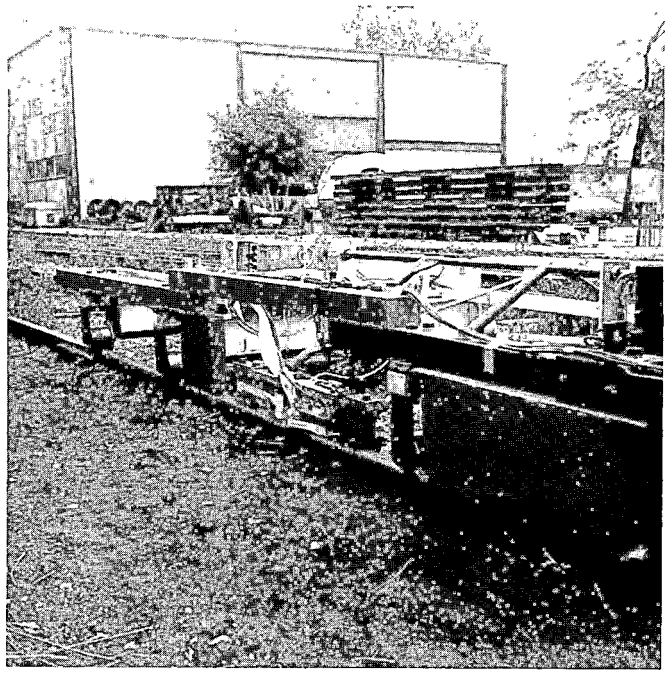

The trailing pole piece is located 6 ft behind the main magnet; it can be positioned also at 9 and 11 ft.

FIGURE 18. VIEW OF RAIL TESTING APPARATUS SET UP FOR CONFIGURATION D

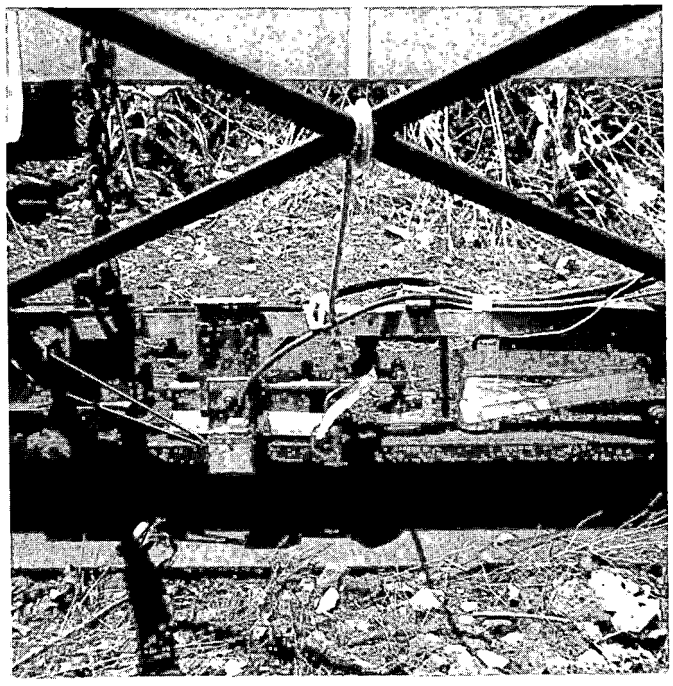

The NOB coil and main pickup box are on the left, the Hall element array in the center, and eddy current probe on the right.

FIGURE 19. CLOSE-UP VIEW OF COMPLETE DETECTOR CARRIAGE ASSEMBLY

6.2 Post-Test Data Reduction and Results

Generally, cursory review of the various test run analog charts indicated the presence of many definite flaw-like signals. The pickup coils consistently showed numerous signals like those from known transverse fissures, compound fissures, shelling, and welds. A more complete check showed them to be both from documented defects as well as from locations where no known flaws were present on available AAR pen-chart records. It was determined that the instrumentation was being operated at a higher sensitivity than AAR customarily was and that we were actually finding more flaws than were documented. A better signal-to-noise ratio existed in our systems for the pickup coil signals than for the Hall element sensors; but the Hall elements responded to the approach (and decay) of joint bars in the region of joints more so than the coils. Lastly, the eddy current sensors were overly sensitive to liftoff, especially at 15 mi/h because the carriage bounced excessively.

A detailed visual examination and study of the analog records for the various sensor channels of selected runs was quite revealing. Numerous short time intervals were selected for viewing on a Nicolet 440A real-time digital spectrum analyzer, as was the associated spectral content of the sample. Combining these previews with adjustable low-pass filtering (LPF) of various sensor signals, especially from the main pickup box coils, it was demonstrated that most of the signal intelligence lay below about 100 Hz (for 4 mi/h). Filtering with a low-pass cutoff of 500 Hz, for example, had no noticeable effect on the signals. A 50-Hz cutoff, on the other hand, reduced the "noise" in the signal but did not seem to have much effect on the intelligence; however, a 1 -Hz Low Pass Filter did definitely remove some intelligence. Examples of the analog records for various rail flaws and defects are shown in Figure 20, where typical amplitude-time histories are given.

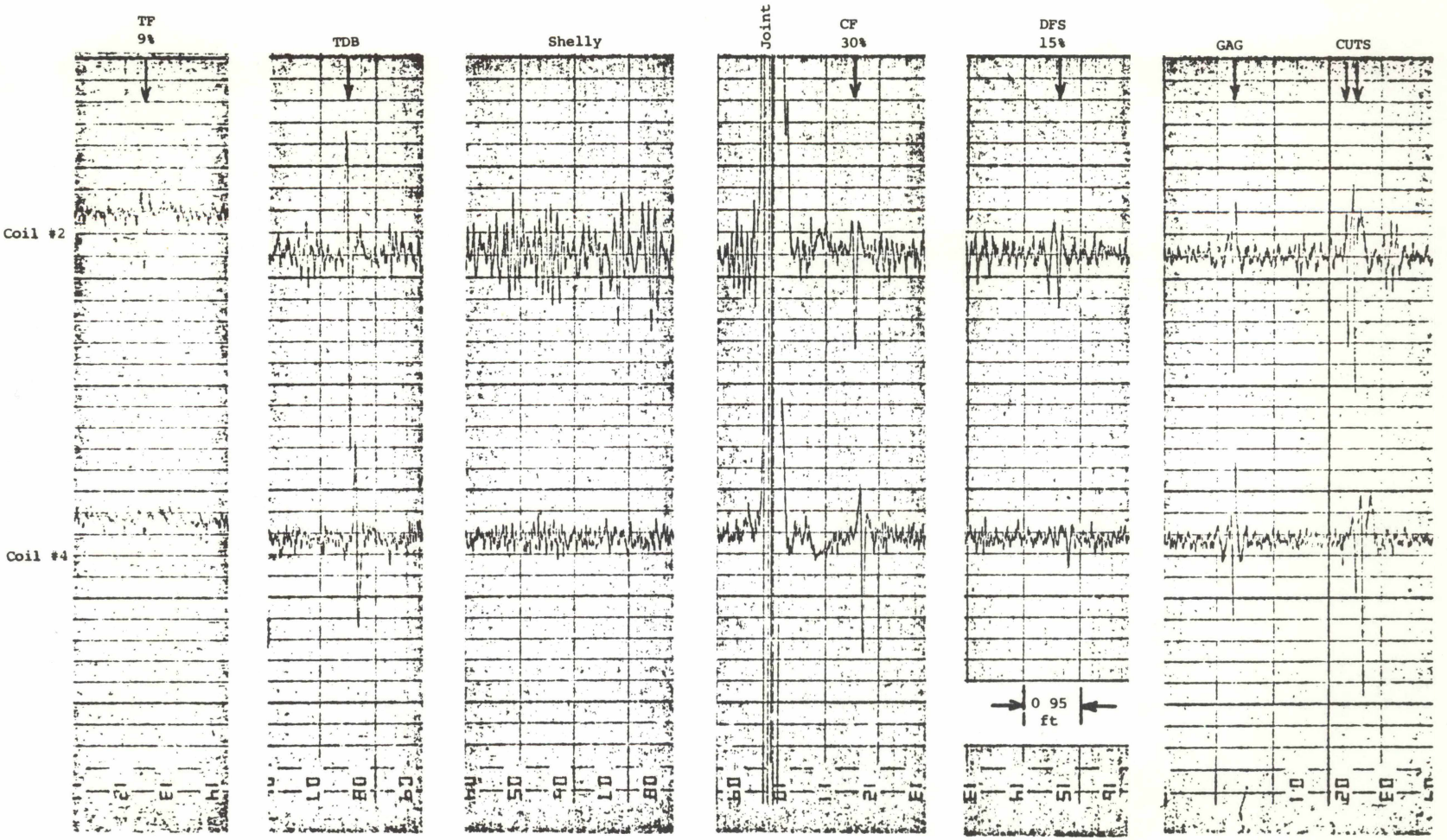

FIGURE 20. SOME TYPICAL AMPLITUDE-TIME HISTORIES FOR VARIOUS RAIL FLAWS AND DEFECTS

Several signal analysis procedures were implemented to aid in identifying criteria for flaw detection and characterization, as well as false signal rejection. The procedures evaluated included such schemes as differentiation, scaling, thresholding (baseline clipping),and modulation. This required digitizing those records of most interest so as to derive appropriate decision algorithms. Experimentation began with the simpler ones in searching for ways to enhance flaws as well as to reduce the effect of extraneous signals such as from the joint bar regions.

The thirty sets of raw data were converted from analog to digital form using a special-purpose program that could drive the analog-to-digital convertor and arrange the digitized output record into an easily accessed file for subsequent manipulation. The details of the digitizing procedure adopted are as follows. Based on preliminary examination/study of the analog records that most of the useful rail defect information seemed to lie below 100 Hz (in the frequency domain) for the test speed of ∿4 mi/h used on the AAR test track, a digitizing (sampling) rate of 120 Hz was chosen. At a velocity of ∿4 mi/h (6 ft/s) for the test run distance of ∿300 ft, the corresponding time is 50 seconds. This amounted to a total of 6000 digitized points per data record.

Digital signal processing procedures were then applied to several such digitized signal records. It became evident early in these signal processing studies that the sampling rate -- one point every 8.3 ms -- was too low to preserve the particular flaw signal characteristics for detection/location; it was thus necessary to return to the task of redigitizing the raw data. Review of the characteristic nature of various flaw types led to the selection of a sampling rate about five times that used at first. (The sampling time was accordingly reduced to 1.7 ms for an equivalent rate of nearly 600 Hz.) A four-pole Butterworth low-pass filter (24-dB/octave rolloff) was used with the cutoff set to 500 Hz to avoid aliasing in the digitized data. The digitizing time length per data track was also shortened somewhat to reduce the total data storage requirements, which were taxed by the increased sampling rate. These changes, in essence, called for nearly five times the machine digital storage capacity (on disk) than initially used; because of storage limitation, only selected data runs could be redigitized to the required precision.

After having obtained sufficiently precise digitized data, the signal processing methods investigated at length included combining routines such as differentiation, scaling, thresholding (baseline clipping), filtering, and modulation. A relatively simple and straightforward method was discovered for reliable flaw detection/location after much experimentation. It involved principally differentiation and thresholding and, sometimes, scaling since the relative sensitivities varied between channels. The signal from a sensor, say a coil for example, was differentiated and the value of the derivative was found large when the signal changed amplitude quickly due to a flaw. The differentiated signal was further "thresholded" to eliminate extraneous information near the baseline.

Figure 21 illustrates a typical computer-plotted result using this analysis procedure on the digitized signal for coil #4 -- the "broad coverage" AAR coil -- showing (a) the coil output signal as it moves along the track, (b) the derivative of this signal, and (c) the derivative thresholded. This record is for the 6-1/2-ft Sante Fe rail section in the AAR test track which contains several transverse fissures cataloged as ranging from ∿5 percent to ∿80 percent of the head area. Their presence is readily noted on the records, with the characteristic discriminator analog signal changing to a schmoo curve upon differentiation, and then "clipped" after thresholding.

It is important to note that the accuracy of this detection method depends critically upon where the threshold level is set, just as is practiced by experienced AAR detector car operators. The baseline level must be varied with the velocity of the sensor and with the ambient noise level. To replace the ad hoc method used presently, a long-term averaging method can be automatically implemented.

That this procedure does indeed work is verified by referring to Table 2 where the locations of the various flaws are noted as scaled from the computer plot and compared to the actual documented positions in the rail. Note that no flaws were missed, but one false alarm appears in the cumputer-processed raw data; this is excellent agreement. The one false alarm would probably be dropped if the threshold were set a little higher.

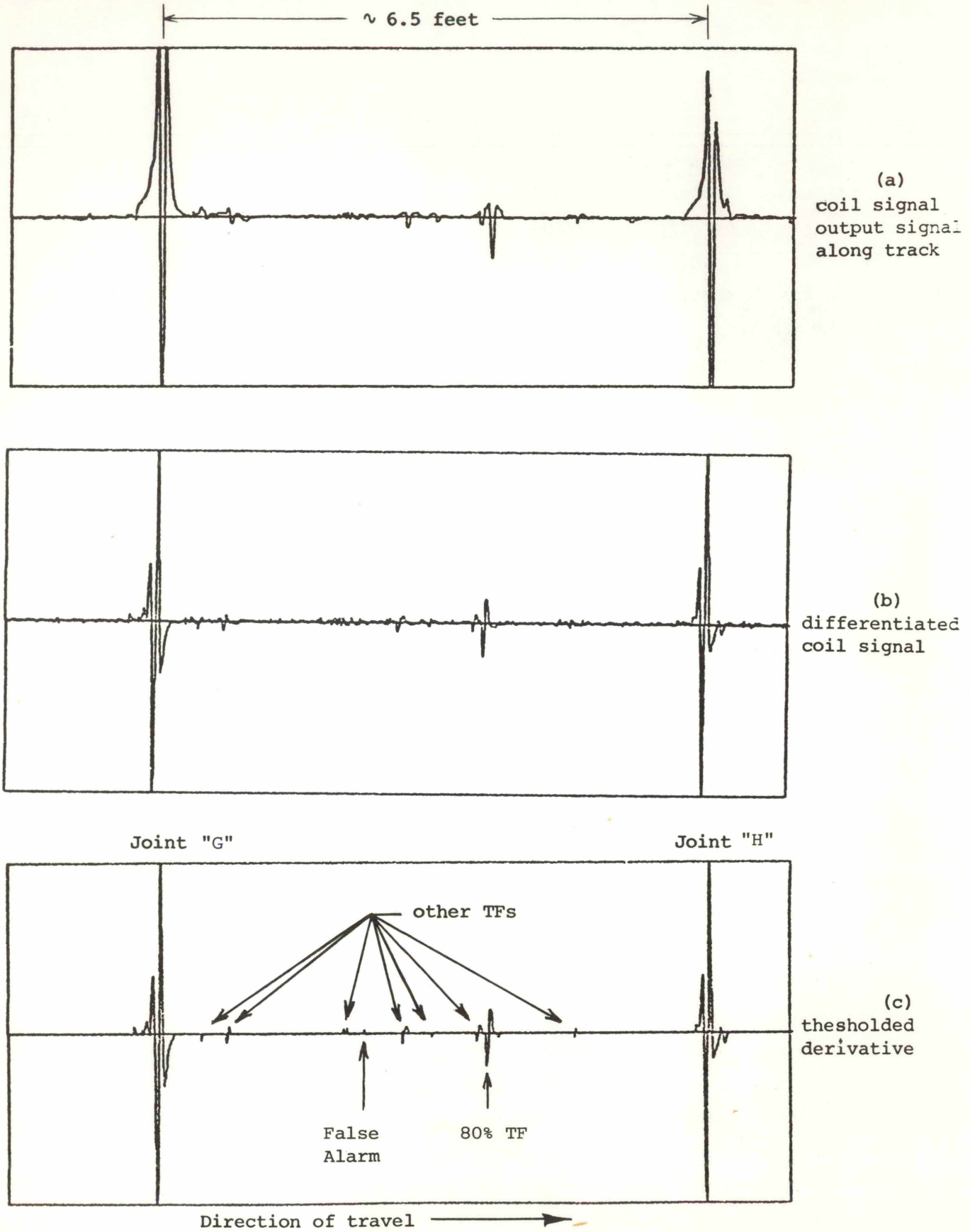

FIGURE 21. AAR COIL NO. 4 SIGNAL AND RESULTS OF SIMPLE PROCESSING PROCEDURES -- SANTA FE RAIL IN AAR TEST TRACK

TABLE 2. COMPARISON OF COMPUTER-PROCESSED RAIL FLAW LOCATIONS AND ACTUAL POSITIONS IN TEST TRACK (6-1/2-ft Santa Fe Rail)

Position from North End of Rail, ft		Flaw Type and Size (% of Rail Area)
Computer-Processed	Actual	
0.55	--	Joint effect
0.85	0.88	TF35%
2.32	2.38	TF15%
2.57	--	False alarm
3.03	3.04	TF30%
3.40	3.40	TF15%
3.98	3.92	TF40%
4.08	4.08	TF80%
5.18	5.17	TF10%

Such signal processing procedures have also been successfully applied to other flaws. The detail fracture is a transverse defect that occurs at the gage corner of the railhead. Figure 22 shows a series of records giving the reconstructed analog signal and the differentiated-thresholded signal for each of the six standard AAR coils. In each case the analog signal is on the left side and the respective differentiated-thresholded signal to its right. Arrows indicate the location of the same known flaw, a detail fracture, on each record if it is visible.

Just a quick glance reveals that the detail fracture is most easily spotted by the NOB and #2 coils, the ones which look directly at the gage corner. For both coils the flaw gives a schmoo type of response which stands out quite well in the processed trace. Continuing across the coils, the effect of the flaw is less noticeable in coils #3, #4, and #5 and disappears entirely in coil #6.

Note that in all of the processed traces the flaw produces an equally positive and negative spike. The amplitude of this spike gives some idea of the size of the flaw and the distance from the coil to the flaw. To positively identify a detail fracture it is necessary to analyze the shape of the signal and the strength of the signal as a function of the various coil positions.

Figure 23 presents a more typical type of transverse defect -- an engine burn fracture. This flaw was documented by AAR as an ordinary engine burn. After hand checking the track with magnetic particle inspection techniques, its true nature was discovered. All of the coils, except coil #5, see the flaw and it generally appears as a schmoo curve. Coil #5 did not pick up this flaw because it is located nearer the gage side of the rail.

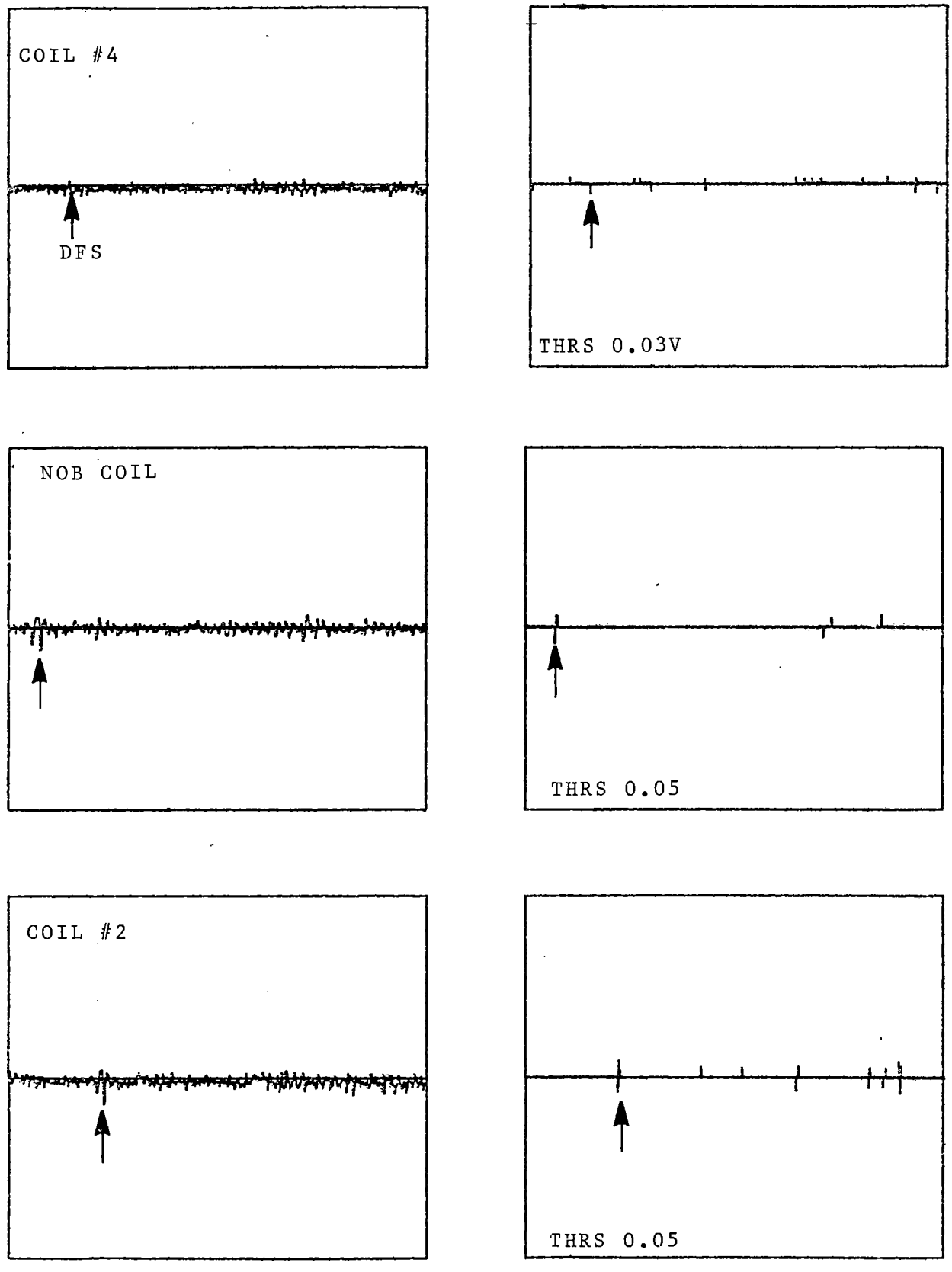

FIGURE 22. AMPLITUDE-TIME HISTORIES OF ANALOG AND DIFFERENTIATED-THRESHOLDED SIGNALS FOR SECTION OF RAIL CONTAINING A DETAIL FRACTURE

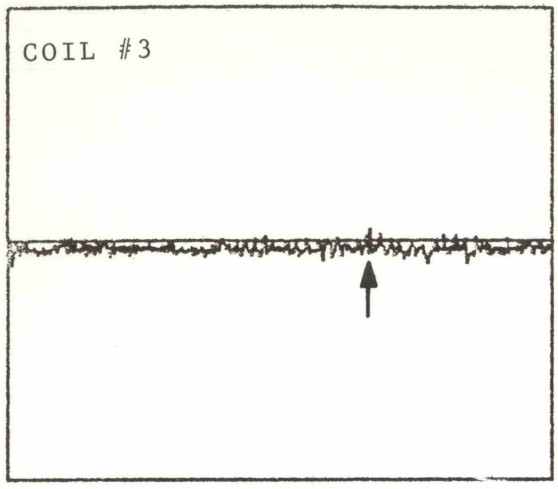

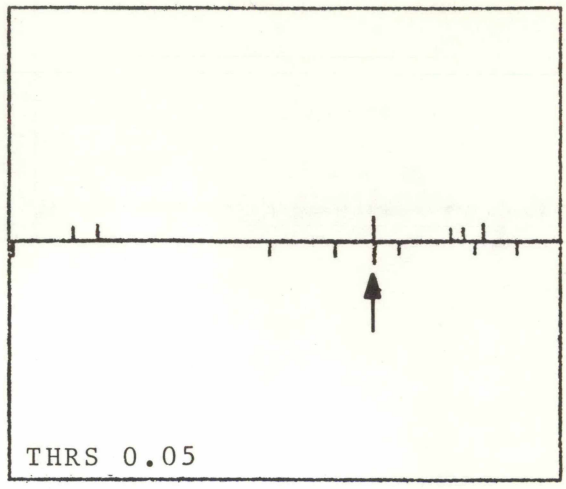

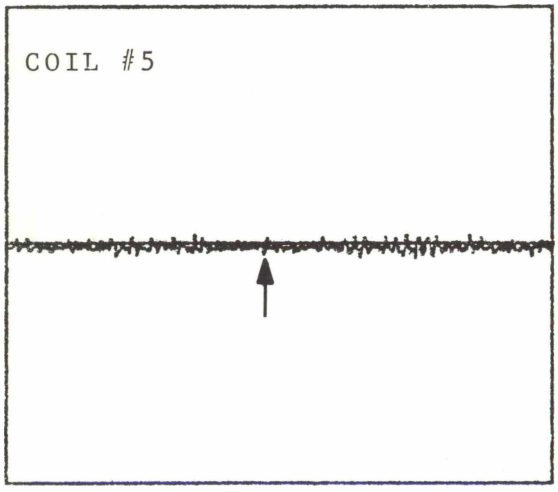

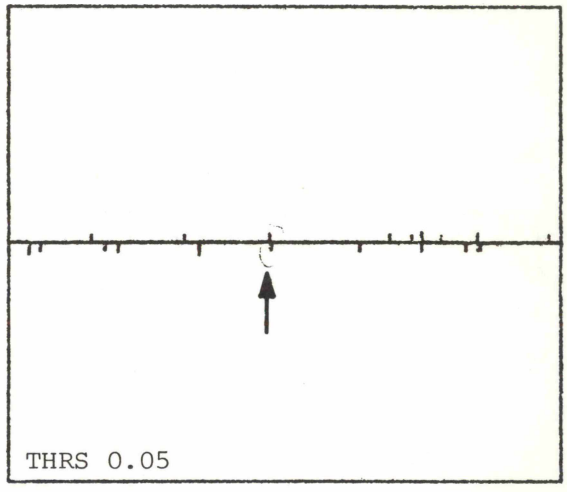

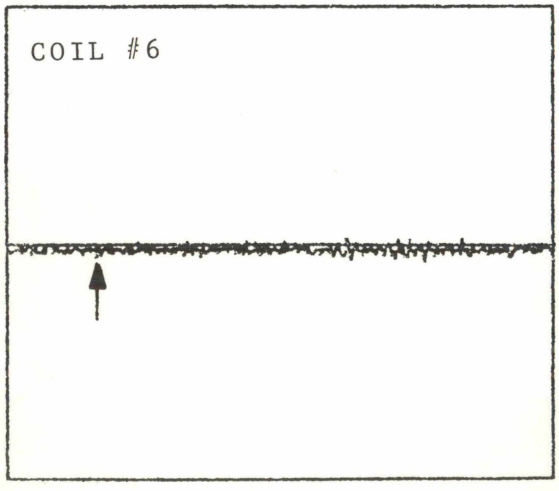

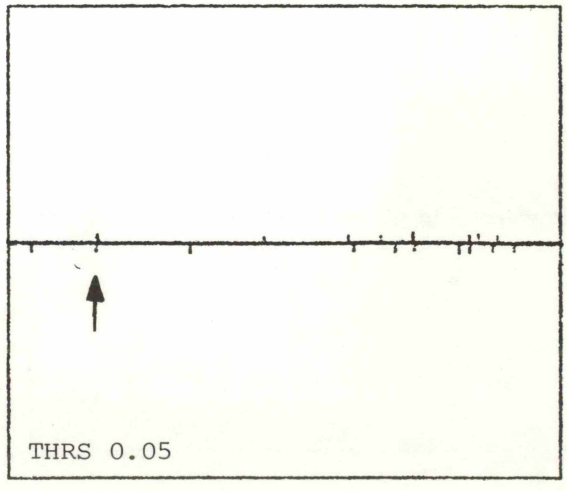

FIGURE 22 (Continued)

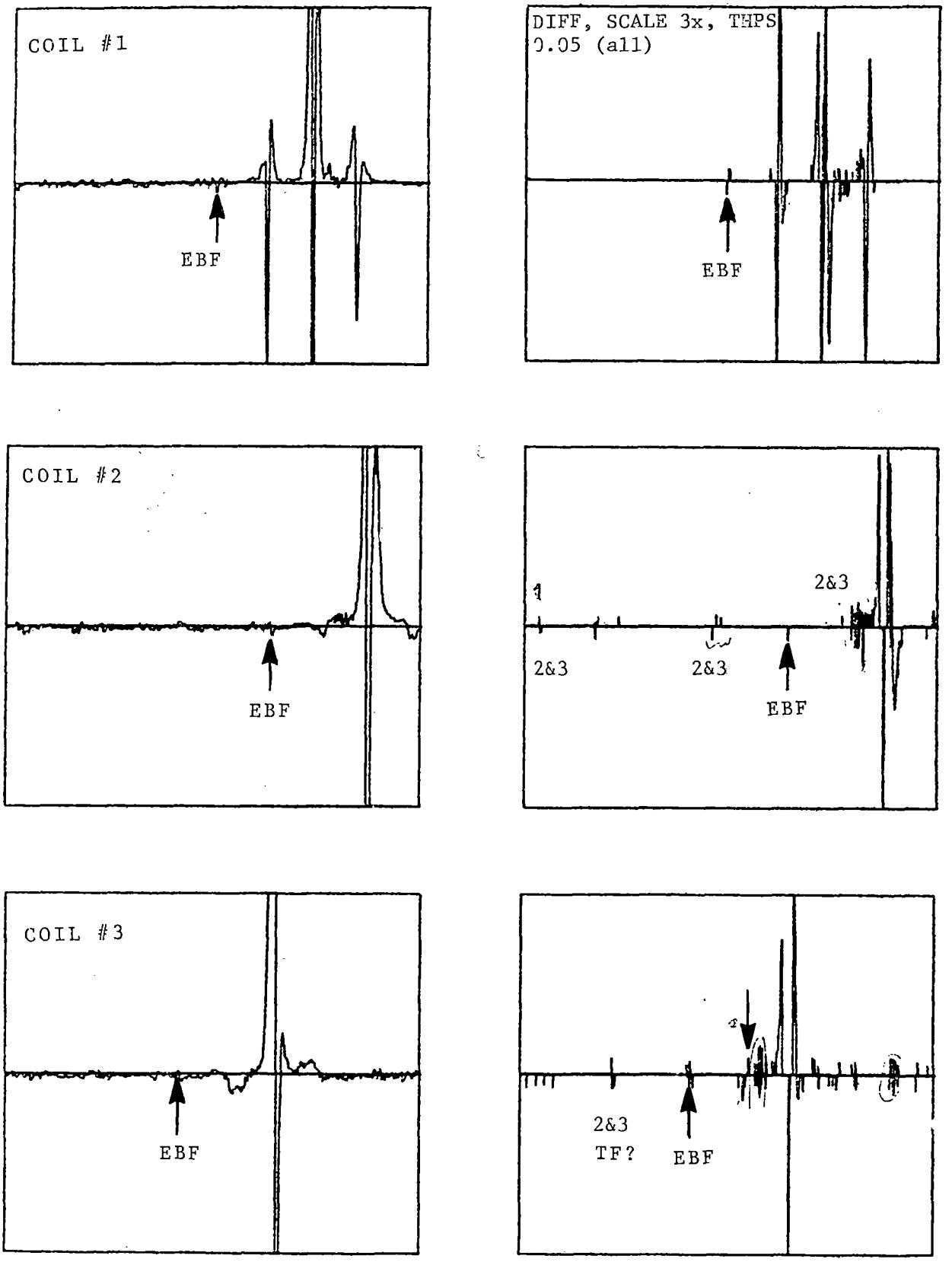

FIGURE 23. AMPLITUDE-TIME HISTORIES OF ANALOG AND DIFFERENTIATED-THRESHOLDED SIGNALS FOR RAIL SECTION CONTAINING AN ENGINE BURN FRACTURE

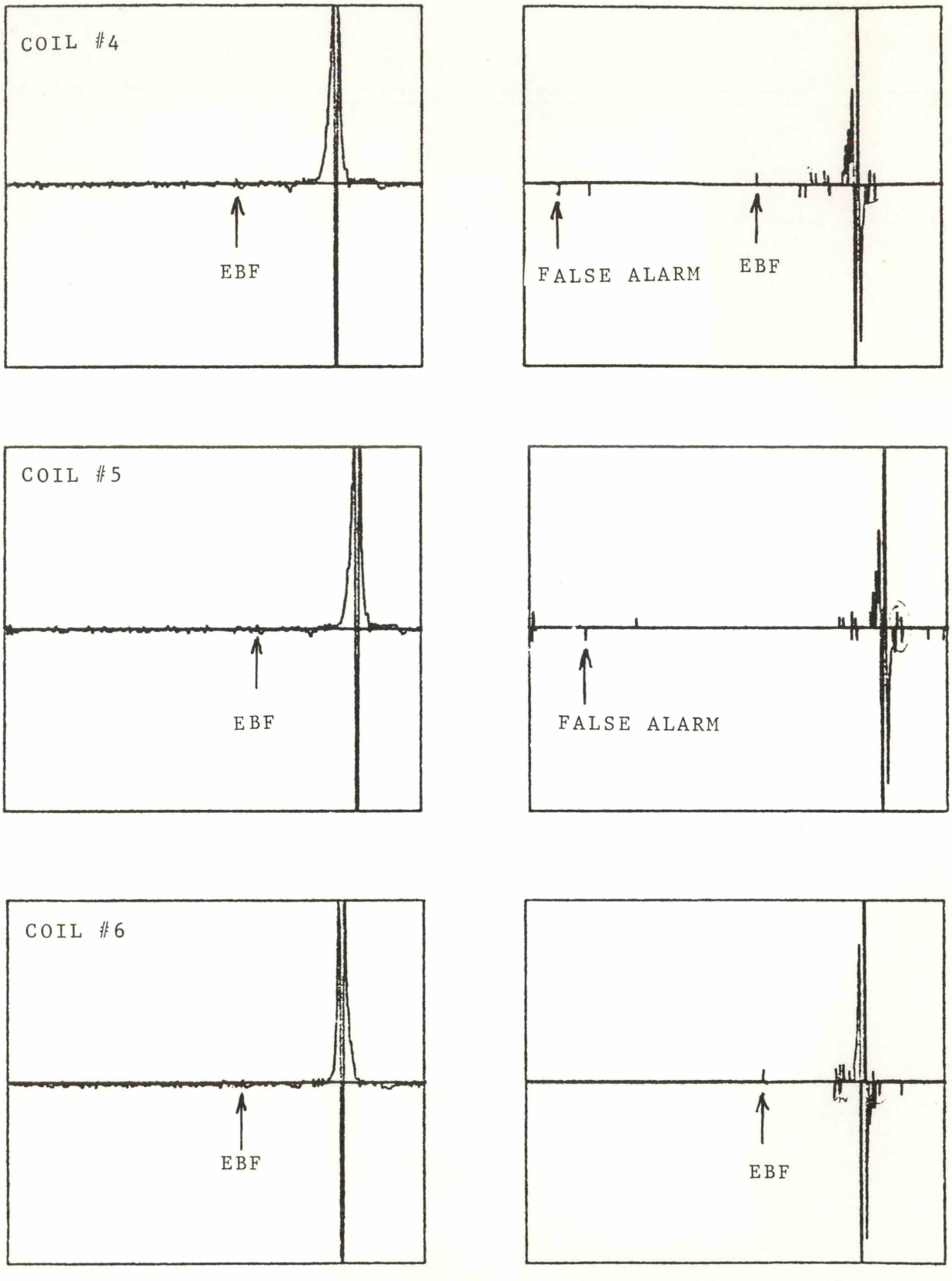

FIGURE 23. (Continued)

Besides this engine burn fracture the coils also spotted another possible flaw within the rail joint region. In most of the processed traces this flaw appears as a series of heavy dark lines near the major excursion of the joint response. The NOB coil does not indicate this flaw. This area was not studied during the hand check so it is impossible to know exactly what the cause of these indications is. From examining a photograph of the area (Joint F), it is possible that the coils are seeing an engine burn, but the locations do not concur exactly.

Appearing at the left edge of the processed traces for coils #2 and #5 is also another flawlike response. This does not show on the other traces due to a time registration difference caused by slight shifts encountered in manually starting the analog-to-digital conversion. Its position does, however, agree with one of the other engine burn fractures verified as existing in the section of rail.

Coils #2 and #3 also indicate a flaw that is not supported by any of the other coils. This is either a false indication or some sort of transverse defect. If it is a defect, then it is extremely small, say under 10 percent, and is located very near the gage corner. It is definitely not a detail fracture since the NOB coil does not detect it. The responses are almost too strong to be noise and far too coincidental, so this indication remains unresolved.

Shown in Figure 24 are (a) the signal output of Hall element No. 2, which is in a plane parallel to the top of the railhead on the gage corner, and (b) the processed (differentiated) Hall signal for the Sante Fe rail. Joints present a strong long-term response, but there is little indication of possible faults, or at least the information is very close to the noise level. Other types of flaws, like transverse defects under welds, do show strong indications and can be detected by the same technique used for the coils, but strangely enough engine burns are not detected.

The lack of sensitivity for Hall elements in detecting transverse fissures and compound fissures can be attributed to the fact that the Hall element responds to <u>changes</u> in the B field and not to the <u>rate of change</u> of the B field as do coils. The difference between the magnetic

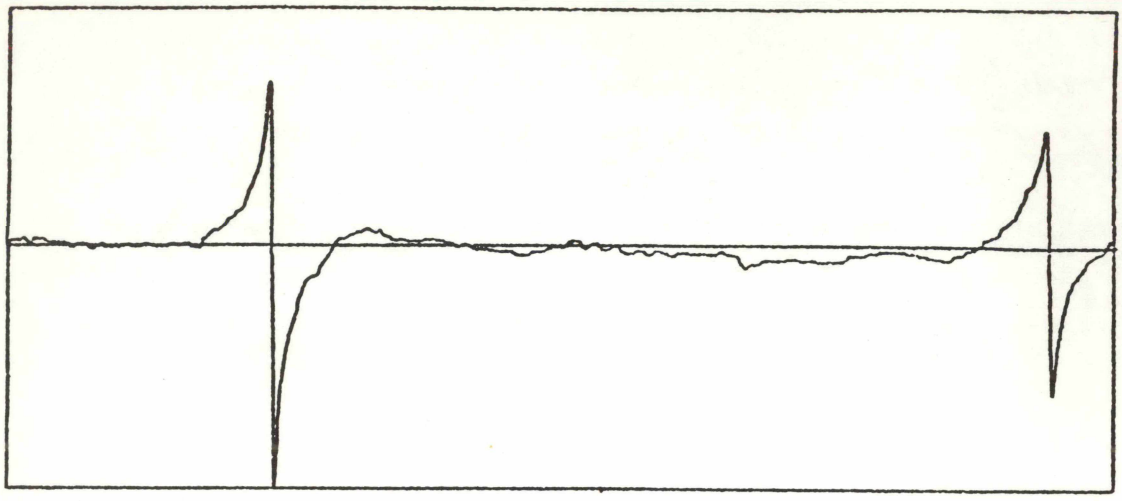

(a)
Hall element output signal along track

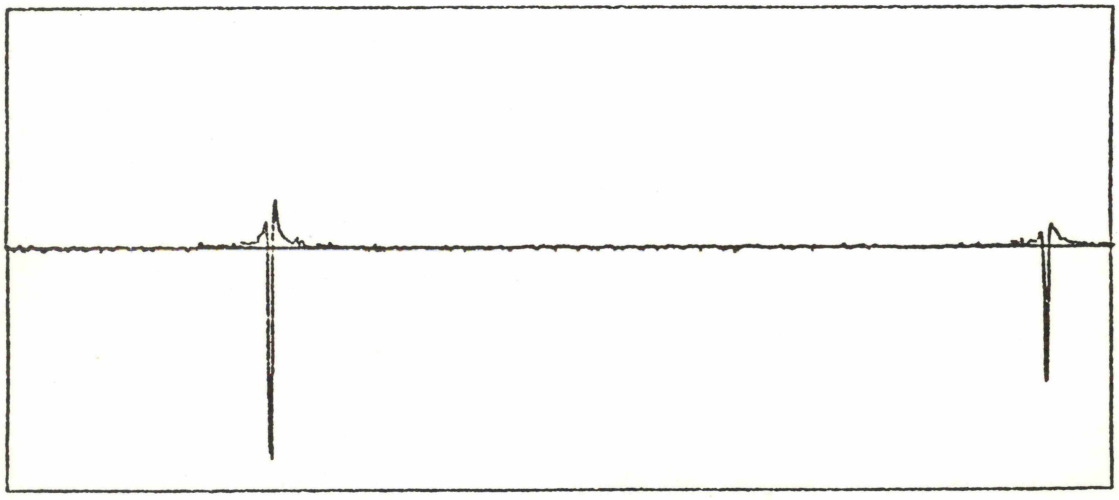

(b)
differentiated Hall element signal

FIGURE 24. HALL ELEMENT NO. 2 SIGNAL AND ITS DERIVATIVE -- SANTA FE RAIL IN AAR TEST TRACK

field strengths over fissures, as compared to the strength of the field elsewhere, is not as great as the suddeness of the change. Other configurations of the Hall elements, such as in either transverse or longitudinal vertical planes, seem to be better at indicating flaws with higher signal-to-noise ratios than the configuration which produced the response for Figure 24. However, Hall elements present distinctly different size and/or types of flaw signals than do the coils.

6.3 Proposed Signal Processing Methods

This difference can be used to great advantage. By examining the output of a coil and a corresponding Hall element, defects can be classified and measured depending on the amplitude, shape, and kind of sensor. Hence, it is conceivably possible to build an automatic classification and recording system. The accuracy of such a system will be dependent on the degree of disparity between the various sensing devices and the accuracy of the basic flaw detection scheme. For example, a threshold system might be employed that dynamically modifies itself to provide a signal-to-noise rejection level that passes only flaw responses. Such a system can be devised by using an integrator whose output is a signal proportional to the average peak-to-peak voltage of the sensor. The integrated signal and sensor outputs are then fed to a comparator, and if the sensor signal is greater in magnitude by some externally set significance level, the comparator will gate the sensor output to a voting network.

To prevent a system-wide noise response from falsely indicating a flaw, a reference detector, situated near the rail environment but not "examining" the rail, can be used as a negator and would cancel all indications if such a noiselike spike occurs on its channel.

To provide for any possible time delays in sensor responses, due either to longitudinal separation of the sensors or because of a peculiar orientation which a flaw might make with respect to the direction of motion, a timer can be initialized when the threshold circuit indicates a possible flaw. Since the holding time is directly related to the velocity of the sensor and the angle of flaw and/or sensor, the time window for voting can be automatically controlled using simple circuitry. For example, a 40-mm flaw canted 45 degrees horizontally with the sensors moving at approximately 6.6 mi/h will require an "open" time of about 10 ms.

Concerning the voting network of the detection system, this accepts the outputs of the sensor timers and will only pass on a response if all the selected sensors "see" the flaw in the same time period. In its simplest form, a voting arrangement can be built using a multiple-input gate arrangement. Careful consideration has been given to which sensors should be connected together. Table 3 lists how we believe the coils of the AAR configuration should be grouped and what each grouping is oriented to detect. Depending on the actual types of sensors employed, e.g., coils, Hall elements, etc., and the area searched, it might be desirable to examine particular sensor outputs directly for flaw responses. For example, the NOB coil can be used independently to indicate shelling.

Besides improving the reliability of the detection system, a means has been found to automatically markout rail joints. The output from a sensor coil can be fed into a low-pass filter and thresholded at about 50 mV. This signal can then be applied to a wave shaper with the final output appearing as a pulse, the duration of which is the length of the joint bars. The voting circuits can be blanked by this pulse or an indication made on the record.

TABLE 3. VOTING ARRANGEMENT (AAR COILS)

Coils	Area Scanned and Type of Defect
NOB and #2	Gage-edge defects including shelling, detail fractures and transverse fissures, joints, burns.
#2 and #3	Gage-side defects including transverse and compound fissures, detailed fractures, and engine burns.
#4 and #6	Gage-side and mid-head defects, including transverse and compound fissures and burns.
#4 and #5	Field-side and mid-head defects, primarly burns but also fissures.
#2, #3, #4, and #5	Overall defects affecting most of the rail head.

6.4 Flaw Detection

Figure 25 illustrates in block form a proposed flaw detection system. The output of one of the sensors is fed through a low-pass filter to remove high-frequency noise. The cutoff point of the filter should change with the inspection velocity. The signal is next differentiated and thresholded and it is also fed into an analog delay line. The differentiator can be a simple operational amplier with an RC network across the input.

The threshold circuit must be able to measure noise signal level and cancel the noise; but this level is constantly changing, the threshold must be readjusted. The best way to implement this is to build a device such as an adaptive filter, i.e., a filter whose characteristics are chosen by comparing the wanted signal with that of the raw signal. For the threshold circuit the adaptive filter would take the raw signal as both the desired and the unprocessed input. An error signal, the output of the filter, would predict what the signal should be doing in the next instant of time, the prediction being based on a least-squares fit of the previous signal inputs. If the actual signal exceeds the predicted signal by a preset amount, say twice, then this response can be considered to be an actual flaw.

Basically, the front end will respond only to input signals with fast rising or dropping edges and which exceed the predicted noise margin. The analog delay line is not involved in the detection scheme *per se*, but it does provide a "snapshot" of the signal that triggered the flaw indication. This device, simply an analog charge-coupled device (CCD), holds samples of the signal just preceding the indication, the length of time being determined by the sampling rate and the length of the CCD register. If a flaw is indicated, the originating waveshape is available for classification measurement and/or display.

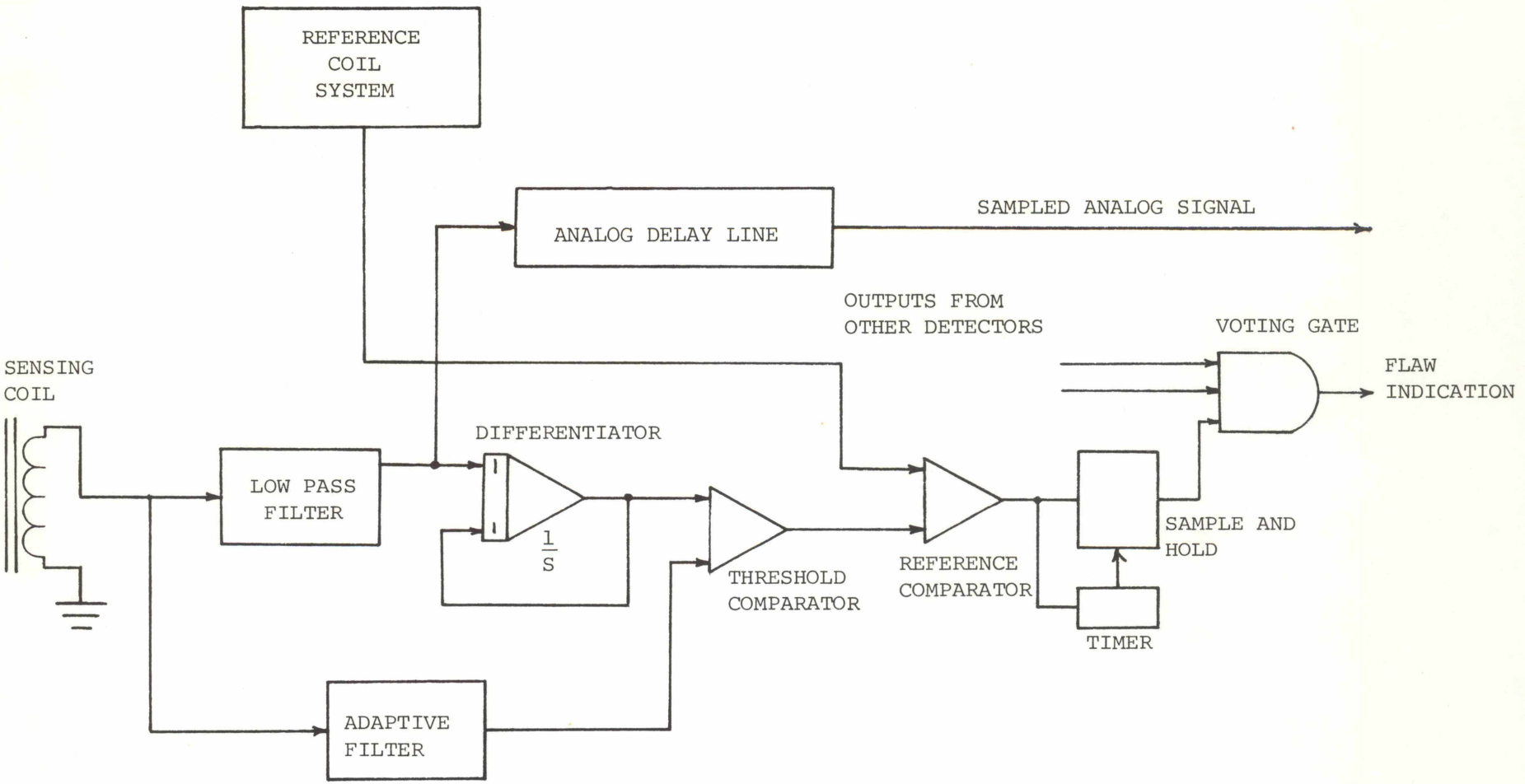

FIGURE 25. PROPOSED FLAW DETECTION SYSTEM

In addition to the single-sensor detection system described above, the reliability can be improved if the outputs of several such detectors are correlated. The best way of accomplishing this is with a "voting" circuit, a circuit somewhat like an AND gate that passes a signal if all of its inputs respond simultaneously. It differs from an AND gate in that the voting circuit must allow for some skew in the responses due to longitudinal separation of the sensors and/or rail flaws. Each input, therefore, needs to have a timer that is started whenever a flaw indication appears. If during the interval that the timer is active one of the other detectors sees a flaw, the circuit will "vote" by producing an output signal. Otherwise the timer will run out and no flaw will be indicated.

Additional reliability can be gained if a noise cancellation system is included with the rest of the processing circuitry. This system consists of a sensing element that is located such that the rail has no effect on its response. The sensor sees only the ambient environment and any signal coming from the device can be considered as noise. The output signal is processed like any of the other detectors except that instead of generating a flaw indication the response is used to blank out the rest of the sensors. In other words, if a large noise spike should enter the system, the noise cancellation circuitry will prevent a false flaw indication. Success of this method is entirely dependent on the location of the cancellation sensor; it must be in the same general location as the rest of the sensors and yet be isolated from the effects of the rail being inspected.

The detection method is relatively simple; there is no need to use a digital computer to detect flaws from just the raw data. The design, complexity, and timing problems of such an approach do not provide any advantage over an all analog approach. The accuracy and error rate of the proposed detection method depend, to a great amount, upon the threshold circuit. As noted, an adaptive filter is the best approach to this device. The only design consideration not yet fully investigated is how to vary the parameters on the filters, delay line, threshold circuit, etc., as the speed of the test vehicle varies. In general, the basic outline is known and only the particulars must be filled in.

After a flaw has been detected, the operator must be notified and the classification system provided with all of the essential signal information. The human interface may take on several forms including strip chart records, a computer driven CRT display or printer output, or even a flashing light. The choice in no way effects either the detector or the classifier. What is critical is how the detector is to provide information to the classifier. As mentioned earlier, the detection circuitry has a delay line that contains the last few milliseconds of incoming signal. When a flaw is indicated, the data are transfered from each of the detectors to the classification system. This transfer should be done under control of the computer to allow it to look at as much data as it requires. The size of the delay line determines how much time is available to the processor before the flaw is confirmed. Classification accuracy depends on how much useful information is available so one can see how important this delay line is.

After finding a possible flaw, then, the following step is to characterize it, i.e., identify what type it is and how large it is. To do this requires a pattern-recognition system, and even a cursory examination indicates that no simple analog method is available to classify the flaws. A digital approach will be necessary, but in order to be successful quite extensive information must be obtained about each and every type of possible flaw. Selected flaws were characterized during the program by visual, ultrasonic, and/or magnetic particle inspection methods since sufficient flaw documentation did not exist for some, and several prominent flawlike signals definitely had to be confirmed. However, because of insufficient time it was only possible to conceptualize a flaw indication system and to define how the flaws can be classified by an automatic means. It was not possible to design, build and test such a system.

6.5 Flaw Characterization

In addition to reliably detecting flaws it is highly desirable to automatically classify and/or measure the size of flaws. The total system would then need little human intervention, thus greatly relieving the operator of burden. To what extent the flaws can be classified automatically depends on how distinctive the sensor signals generated by each type of flaw are relative to all others.

As seen earlier, rail defect signals fall roughly into two categories, the discriminator and the schmoo curves. (See Figure 6.) Transverse defects, i.e., transverse fissures, detail fractures, rail joints, and welds, yield a schmoo curve when sensed by a coil. These same flaws produce a discriminator curve when sensed by a Hall element. On the other hand, compound fissures sometimes respond like transverse fissures, but at other times they generate a discriminator response. Vertical split heads do not produce either of these two curves and are thus difficult to identify.

Another flaw that is difficult to spot is the engine burn. In some runs, where the track is highly saturated, a long-term upswing is found to corrspond with some of the burns, but not all of them. Careful analysis has shown that some of the engine burns in the AAR test track actually had fractures associated with them, but had not been previously identified as such by AAR detector car operators. Several specimens of the test track have engine burns that have been cleaned out and filled in by weldment. Both the coils and the Hall elements clearly indicate the welds. One of these welds had a transverse defect beneath it which shows as a very large spike in the Hall element recordings. Also of interest is one section of rail which actually consisted of two pieces butt-welded together with an open bolt hole on either side of the weld. When the sensors ran over this piece, the weld and both the bolt holes were indicated!

It has not been emphasized but perhaps the most important clue to identifying the type of fault is not what the output of a sensor looks like, but rather which one of the sensors sees the flaw. For example, if the sensors observing the gage corner of the rail see a flaw

with a schmoo response and the other sensors from mid-rail out see nothing, then it is quite likely that the flaw is a detailed fracture. Similarly other patterns can be discerned that uniquely identify the other types of flaws.

This then leads to a most important question: can the flaws be classified automatically? From what has been observed on the program, the answer is tentatively "yes", if the requirements are not very stringent. Classification can be by several means, but the most promising is to look at the responder pattern then at the actual signal shape. A statistical analysis tree could be used to sort out a recommended route. The best approach seems to be a "seat of the pants" method where the signal is compared against a set of standards such that the one that fits best is the type of flaw encountered. Of course, a lot of compound fissures are going to be called transverse fissures, but this kind of error can be tolerated. Calling a good section of track flawed, when it is not, is unacceptable. The accuracy of the second approach depends on the amount of data collected, the detail to which it can be measured, and the skill of the programmer/analyst.

The only limit to this system appears to be processing speed. If a large number of signals must be scanned then the rate will be lower than if only a small number have to be examined. Thus we have a tradeoff between speed and accuracy. Also the method depends on getting a reasonably sized "snapshot" of the signals for the various sensors.

Inclusion of a classification system will definitely be an improvement over present systems. Even if only rudimentary classification can be made, the need for constantly stopping to hand inspect the rail will be substantially reduced if not entirely removed. Provisions can also be made for self improvement. Assume that the classification system spots a flaw it cannot identify; the operator is notified and the data recorded. At a later date the rail section may be taken up and the flaw positively identified. Corrections to the program can then be made to include this new type of flaw. Besides noting what a flaw may be, the classification system might also be able to measure size at least to the point of saying greater than 40 percent, 20 percent to 40 percent, or less than 20 percent. The key to the problem lay in gathering data from carefully measured rail flaws.

6.6 Rail Magnetization Experiments

The effectiveness of the various rail magnetization techniques was evaluated experimentally. The active field methods tested at AAR appeared overall to work somewhat better than the AAR (residual field) method; all of the flaw responses that were present in the AAR configuration also appeared in the active field runs. The only discernable difference was a change in amplitudes of the responses and the signal-to-noise ratios. Also, in the case of transverse magnetization, vertical split heads could be seen by both the coils and the Hall elements. (This occurred, however, because of insufficient demagnetization, i.e., "removal" of the longitudinal residual field, prior to running with transverse magnetization, as noted below.)

In comparing the various methods, it had been noted in early review of the analog records that after each run the rail retained some residual magnetization. This apparently occurred even though the test cart was backed over the rail with the magnetizing field reversed and reduced to one-half its normal strength as customarily done. Review of the data from several runs performed each day revealed that the residual magnetic field increased significantly with each run and the responses seemed to gain amplitude. Hence it is hard to say exactly what the relative signal strengths are between runs. This is most dramatically demonstrated in the transverse magnetization tests where all of the transverse flaws as well as the longitudinal flaws appear, yet theoretically only the longitudinal flaws should be detectable.

The magnetizing field laid down in the rail was investigated experimentally on the AAR test track statically and for various pole spacings and speeds. First of all, the residual magnetism was measured by inserting a Hall effect gaussmeter probe directly into the gap between rail ends in several rail joints. Although the test track had not been magnetized for several months, the joint gap flux density typically found was between 80 and 100 G. The higher value existed in the outer

regions of the railhead, especially at the upper and lower corners both on the gauge and field sides. The lower value corresponded to the base of the head at the web; intermediate values were found in the central region of the railhead. Flux levels of 30 to 50 G were present in the trackage over which the magnetic rail inspection equipment had passed to gain access to the test track, and this trackage had not knowingly been magnetized. The AAR test track* is situated along a north-south line, and is not used except for storing rail cars on an as-needed basis. As such, it is not subjected to the traffic a mainline is. It is the experience of AAR rail detector car operators that rail gap flux density may typically be no more than 10 to 15 G after routine inspection of mainline. Further, it is "knocked down" to one-half these values in hours or days after magnetizing, depending on the amount and type of traffic using the line. More frequent use by heavier traffic leads to faster decay of the track residual field, although in actuality the rail never reaches a demagnetized state.

The magnetic field retained in the AAR test track was investigated further after removing the joint bars at Joint "J" midway in its 400-feet length were the railhead gap was typically 3/8 inch. Figure 26 shows this joint after the joint bars were removed. Over the head area the flux density was found to vary between 1050 G along the upper edge to nearly 1500 G along the lower edge. It varied from 1500 to 1800 G in the web, and even exceeded 2000 G in the base. These residual values suggest that the rail had, in fact, been magnetized to saturation. (Recall that the rail had not been magnetized for several months, at which time it was supposedly demagnetized.) Obviously the rail retained a very high level of residual field, i.e., >1000 G everywhere over its cross section. This joint was then instrumented with both the gaussmeter probe and another Hall probe for making recordings of the gap flux density under different circumstances. These probes were located at the center of the head area where the residual field was typically 1250 G.

---

* See Appendix A for details on AAR test track.

FIGURE 26. JOINT "J" IN AAR TEST TRACK

First attempts to demagnetize the rail by positioning the test apparatus (set for longitudinal magnetization with an 11-1/2-ft pole spacing) over the rail gap were not successful. Although the measured gap field could be cancelled out with a reversed applied magnetic field, and even reversed itself, the residual in the remainder of the rail length was sufficient to return the gap field to about 400 G upon reducing the applied field to zero. Repeated attempts to demagnetize the rail by backing down the track with a reversed field direction of one-half the strength of the magnetizing field were also unsuccessful. It was thus determined that changing both the field direction and the direction of travel over the rail resulted in a reinforcement of the residual field, regardless of its original direction. Finally, a satisfactory technique was found whereby the residual field in the rail could be reduced to less than 100 G. This consisted of magnetizing the rail in the forward direction at the nominal magnetomotive force of ∿18,500 ampere-turns, and then reversing direction at 10 mi/h with only one-sixth this force of the same polarity.

Having found a method to obtain consistent demagnetization of the rail, the flux density in the opened joint was determined for the ∿18,500-ampere-turn magnet with pole spacings of 6, 9, and 11-1/2 ft at speeds of 4, 10, and 15 mi/h. The results of Figure 27 were obtained. Note that the gap -- and thereby the rail -- residual magnetism (flux density) increases as the magnet pole spacing increases and the speed decreases. This is as expected. Four repeated runs at 15 mph for the 11-1/2-ft spacing resulted in a spread of only 40 G for the final value (1280 G), even over the wide range of beginning remanent magnetism from -730 G to +960 G. One point is also shown for the 6-ft pole spacing at a speed of ∿23 mi/h; this appears to fall in line with the lower-speed points. (Further attempts were not made to determine the residual flux density at such speeds because of the potential hazards to personnel and equipment resulting from derailment.) Our rigid-frame cart was not designed to be run at such speeds, but it was believed

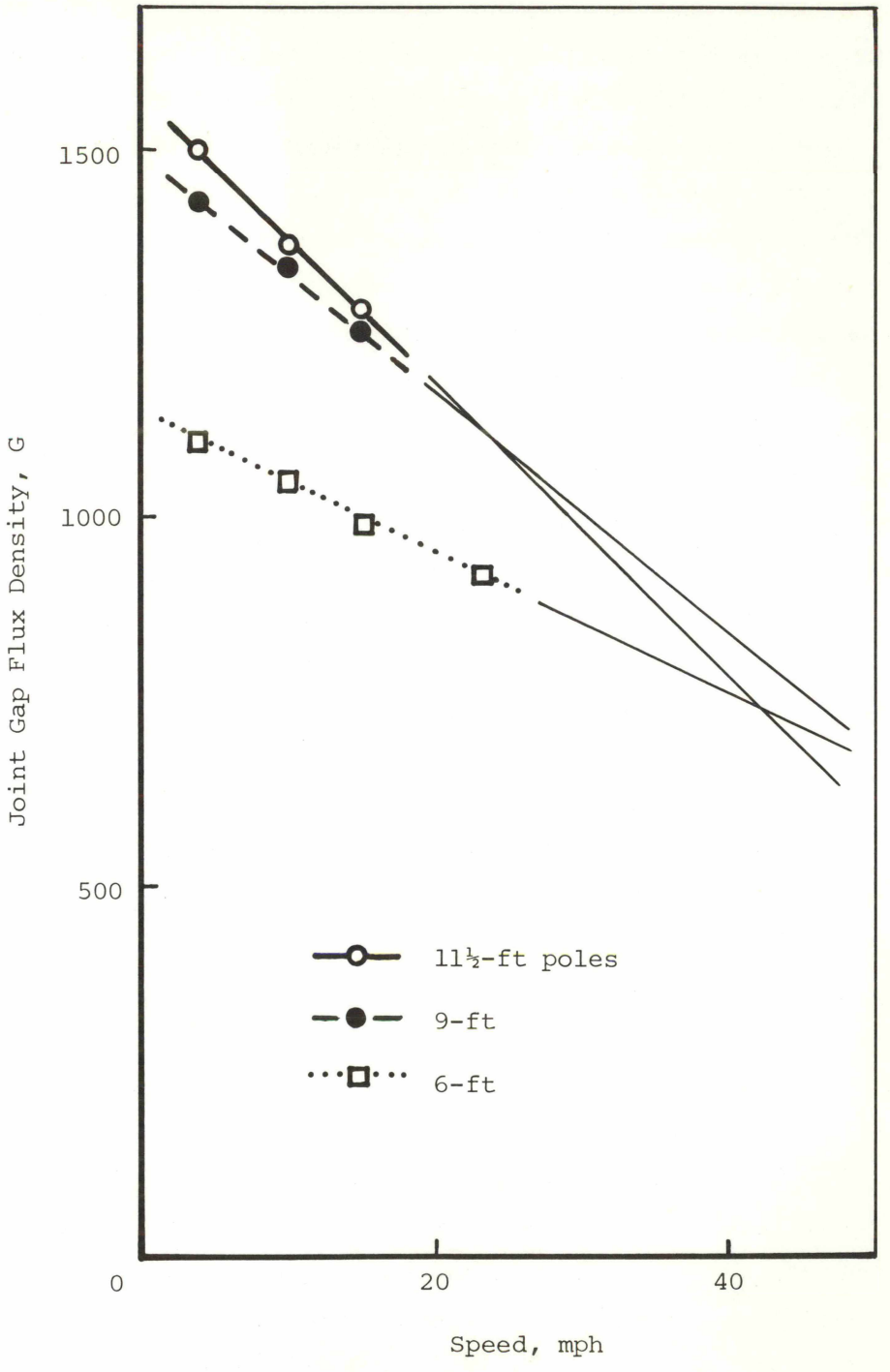

FIGURE 27. RAILHEAD RESIDUAL MAGNETISM AS A FUNCTION OF SPEED -- ACTIVE LONGITUDINAL MAGNETIZATION

worth a chance to attempt to at least get one point at ∿25 mi/h. A significant observation can be made from Figure 27: extrapolation of the flux density of ∿700 G would result at speeds of 40 to 50 mi/h. This assumes the extrapolation to those speeds is valid and that it does not decrease faster at increasing speeds, i.e., droop. A residual flux density at the center of the railhead of 700 G, or so, should be respectable for magnetic rail flaw detection.

In summary, the active magetizing field configuration used (longitudinal) is potentially better than the residual magnetic method. Sufficient magnetizing fields have been applied for this configuration to be demonstrated at ∿25 mi/h, and it shows potential for working at 40 to 50 mi/h, The most sensitive sensors used are pickup coils which respond to the derivative of leakage flux fields at defects.

REFERENCES

(1) Rail Defect Manual, compiled by Sperry Rail Service, a division of Automation Industries, Inc. (1964).

(2) "Sperry Improves its Rail Test Cars," Railway Age, May 9, 1966.

(3) C.N. Owston, "The Magnetic Flux Leakage Technique of Nondestructive Testing," British Journal of NDT, Vol. 16, No. 6, November 1974.

(4) F. Foerster, "Theoretical and Experimental Developments in Magnetic Stray Flux Techniques for Defect Detection," British Journal of Nondestructive Testing, Vol. 17, No. 6, November 1975.

(5) F. Foerster, "Defect Inspection of Hot-Roller Steel Bars without Discaling," NDT International, Vol. 9, No. 6, pp 285-289 (December 1976).

(6) V.V. Vlasov, "Research on the Detection of Railway Line Defects in Moving Magnetic Fields," from Fizika Metallov i Metallovedenie,* Vol. 5, No. 3, pp 442-451 (1957).

(7) ibid., Vol. 6, No. 1, pp 74-81 (1958).

(8) ibid., Vol. 6, No. 2, pp 247-254 (1958).

(9) ibid., Vol. 6, No. 3, pp 426-432 (1958).

(10) ibid., Vol. 6, No. 4, pp 628-632 (1958).

(11) ibid., Vol. 6, No. 5, pp 794-803 (1958).

(12) ibid., Vol. 6, No. 6, pp 1006-1010 (1958).

(13) ibid., Vol. 7, No. 1, pp 159-160 (1959).

(14) ibid., Vol. 7, No. 2, pp 186-191 (1959).

(15) ibid., Vol. 7 No. 2, pp 319-320 (1959).

(16) ibid., Vol. 7, No. 3, pp 341-349 (1959).

(17) ibid., Vol. 7, No. 3, pp 455-457 (1959).

(18) ibid., Vol. 7, No. 4, pp 527-533 (1959).

(19) ibid., Vol. 7, No. 5, pp 789-693 (1959).

(20) ibid., Vol. 7, No. 6, pp 837-841 (1959).

* Physics of Metals and Metallography.

REFERENCES (Continued)

(21) ibid., Vol. 7, No. 6, pp 937-939 (1959).

(22) W. K. Kaiser et al., " Rail Inspection Systems Analysis and Technology Survey," Report No. FRA/ORD-77/39, U.S. Department of Transportation, Federal Railroad Administration, Washington, D.C. (March 1977).

(23) B. P. Dovar and V. A. Schcherbinina, "Investigation of the Defect Fields in High-Speed Electromagnetic Testing of Rails," translated from Defektoskopiya*, No. 1, pp 32-40 (Jan.-Feb. 1965).

(24) B. P. Dovnar, Yu. D. Sychev, V. A. Schcherbinina, and L. P. Ol'shanskaya, "Evaluation of the Surface Effect and the Appearance of Internal Defects in Railheads with Rapid Magnetic Defectoscopy," translated from Defektoskopiya,* No. 3, pp 1-7 (May-Apr. 1973).

(25) B. P. Dovnar, V. V. Vlasov, and V. V. Schcherbinina, "Experimental Investigation into the Dynamic Field of a Defect During the High-Speed Electromagnetic Defectoscopy of Rails," translated from Defektoskopiya,* No. 2, pp 21-27 (Mar.-Apr. 1973).

*Defectoscopy

APPENDIX A

FLAW DETAILS OF THE AAR TEST TRACK

The field experiments conducted during this program were carried out at the Association of American Railroad's site in Chicago where their 400-foot test track is laid. The track had been assembled with just about every conceivable rail flaw. The flaw documentation initially supplied consisted of the standard AAR detector car pen chart records (five channels plus VSH channel). Figure A-1 shows a portion of such a record. The scale of the chart is approximately 1/16-inch to 1 foot, so the record in Figure A-1 is for about 50 feet of track. The upper set of records is for one rail; the lower, the other rail. As can be seen, the right hand side of the lower (west rail) record notes the locations of several transverse defective welds, whereas the central portion has many good weld indications marked. The upper (east rail) record indicates a section of rail having much shelly over its 30-foot length. As can be seen, the AAR test track contains an unusual concentration of flaws. Table A-1 presents data on the west rail of the AAR test track, particularly on the type, size, and location of the defects.

Figures A-2 through A-4 show views and closeups of selected portions of the test track. Figure A-2 shows the 6.5-ft "Santa Fe Rail" (GH), a section of track having numerous transverse fissures from 3 to 80 percent of the head area. All these TDs are internal, except for one that has broken through to the surface. The flaw size data derives from an empirical hand checking method which H. Keevil developed many years ago. It is a regenerative system based on the "current depression" occurring between two heavy-duty test probes about 1/2-inch apart held in good contact with the railhead so as to cause somewhere between 300 and 1000 A (direct current) to flow "around" the internal defect. Over many years of experimenting, this system was refined to the point where the size of internal defects could be determined credibly; confirmation was by correlation of the current depression with the actual size (area) of the defect as determined after breaking the rail open.

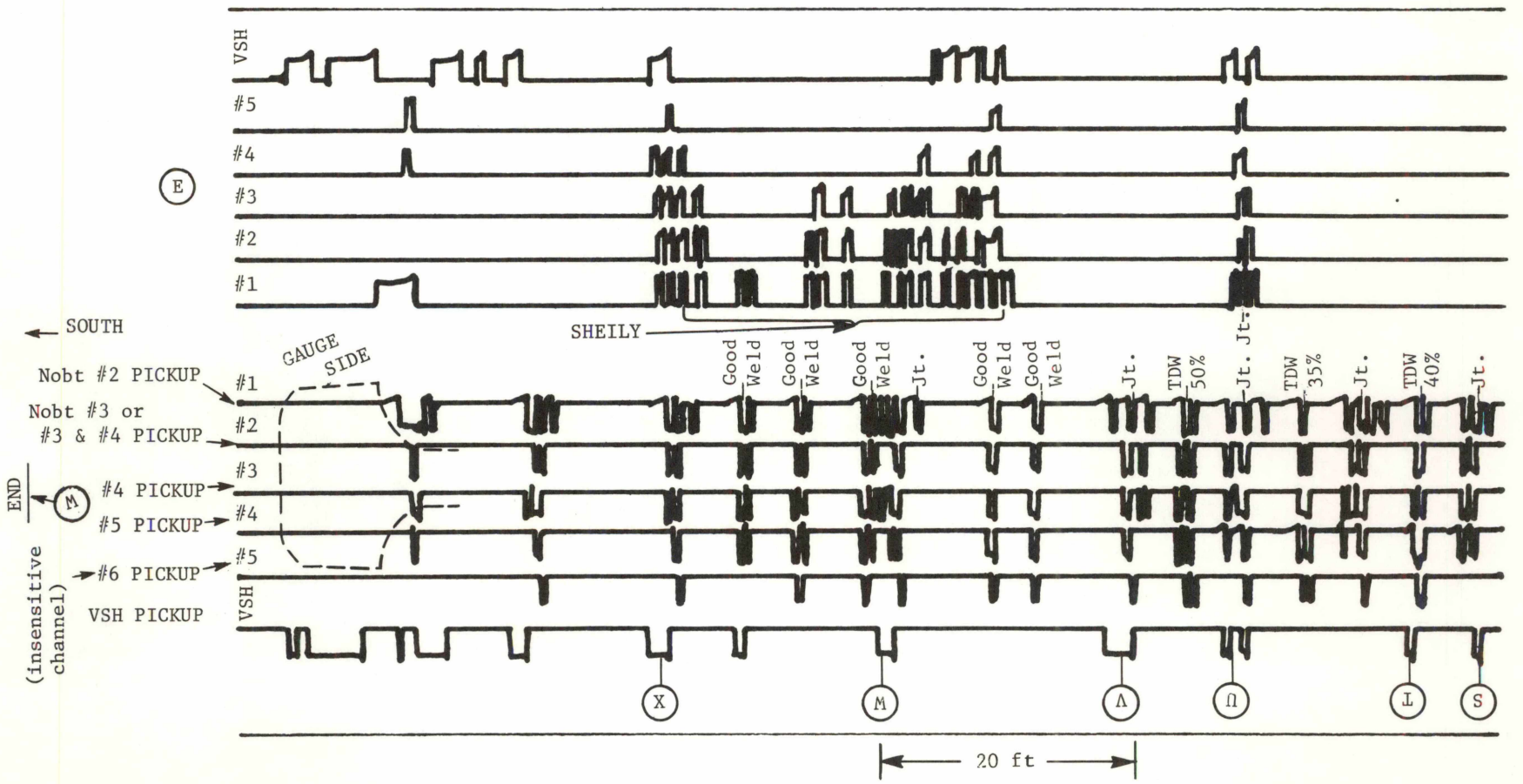

FIGURE A-1. AAR RESIDUAL MAGNETIC RAIL DETECTOR CAR PEN CHART RECORD

TABLE A-1. DATA ON AAR TEST TRACK (WEST RAIL) USED IN PROGRAM

Joint		Rail Section		Defect		
Letter	Bar Length, in.	Size, lb	Length, ft.	Type[a] and Size[b]	Position from Joint, ft.	Notes
C	24					
		100	19.62	TF9	11.06	
D	24					
		100	19.53	TF5	11.52	
E	24					
		110	20.72	B	0.55	Intermediate Mn rail
				EBF[c]	2.79	
				B	3.63	
				B	6.17	
				EBF[c]	6.88	
				EBF[c]	7.29	
				EBF[c]	8.38	
				EBF[c]	10.04	
				B	10.46	
				B	12.83	
				EBF[c]	13.96	
				EBF[c]	18.50	
F	24					
		110	10.16	Nick	5.08	3/16-inch wide, at gage corner
				B	8.04	
G	24					
		110RE	6.81	TF35	0.88	"Santa Fe Rail"
				TF15	2.38	
				TF30	3.04	
				TF15	3.40	
				TF40	3.92	
				TF80	4.08	
				TF3	4.92	
				TF10	5.17	
H	24					
		110RE	17.41	TF12	3.31	
				TF8	10.00	

TABLE A-1. (CONTINUED)

Joint		Rail Section		Defect		
Letter	Bar Length, in.	Size, lb	Length, ft.	Type[a] and Size[b]	Position from Joint, ft.	Notes
I	24					
		110	18.94	BH	4.79	Intermediate Mn rail
				CF40	5.83	
				BH	6.38	
				EBF[c]	14.42	
				B	14.92	
				B	15.92	
J	24					
		110	20.00	B	2.23	
				B	4.38	
				TDB[c]	7.88	
				B	9.96	
K	24					
		110RE	39.00	HSH	8.33-8.75	"Shelly" Rail
L	24					
		110	11.54	B	3.31	
				VSH	4.38-6.00	
M	WJ[d]					
		100	6.43	VSH	1.73-4.50	With 16-in. plates
				B	2.54	
N	WJ					
		110	21.07	CF30	1.68	
				CF35	19.34	

TABLE A-1. (CONTINUED)

Joint		Rail Section		Defect		
Letter	Bar Length, in.	Size, lb	Length, ft.	Type(a) and Size(b)	Position from Joint, ft.	Notes
O	24					
		110	8.71	CF(c)	3.96	
P	WJ					Joint fractured; with 16-in. plates
		110	4.33	G	∿2.0	
Q	WJ					With 16-in. plates
		110RE	17.97	DFS15	4.29	
R	24					
				G	6.71	
				Cut	8.98	1/4 w x 3/16 d
				Cut	9.13	1/4 w x 3/8 d
				G	14.58	
				G	17.08	
				G	23.54	
S	24					
		132	9.94	TDW40	4.87	
T	36					1-in. rail gap
		119	10.21	TDW35	5.04	
U	36					
		119		TDW50	5.00	
V	36		10.01			
		119		--	8.00	Good weld
				--	11.60	Good weld
W	36		19.54			
			Σ = 330 ft			

(a) Defect type classification is as follows:
- B - burn (surface anomaly)
- BH - bolt hole (no cracks)
- CF - compound fissure
- DFS - detail fracture from shelling
- EBF - engine burn fracture
- G - corrugation (mill defect)
- HSH - horizontal split head
- TDB - transverse defect from engine burn
- TDW - transverse defective weld
- TF - transverse fissure
- VSH - vertical split head

(b) Size, e.g., 35, is percentage of head area.
(c) Size undetermined.
(d) Welded joint.

FIGURE A-2. THE AAR "SANTA FE RAIL"

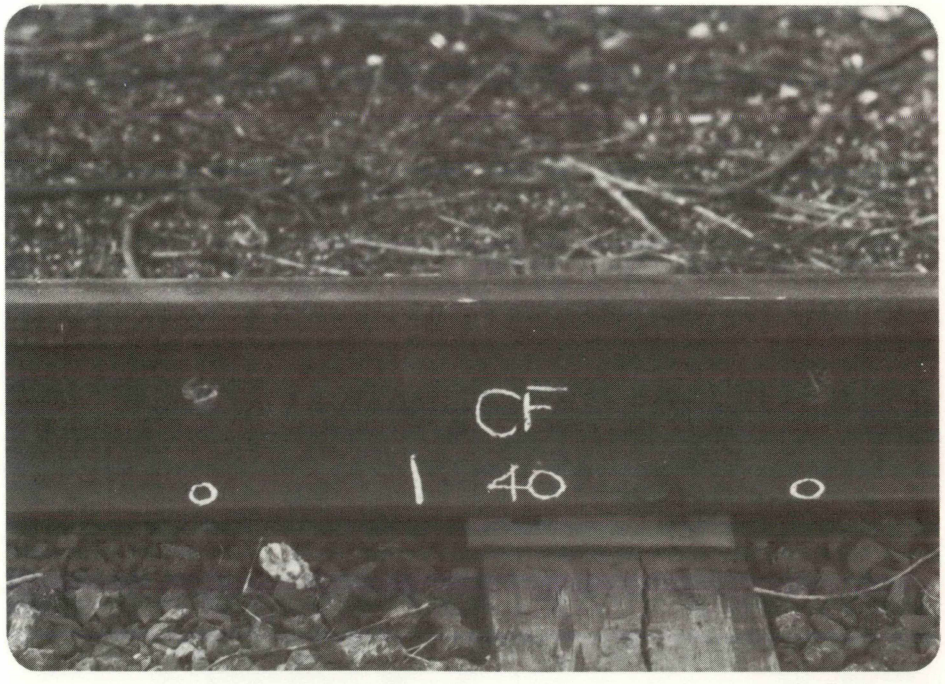

FIGURE A-3. PORTION OF RAIL IJ SHOWING RELATIVE POSITIONS OF BOLT HOLES AND A COMPOUND FISSURE

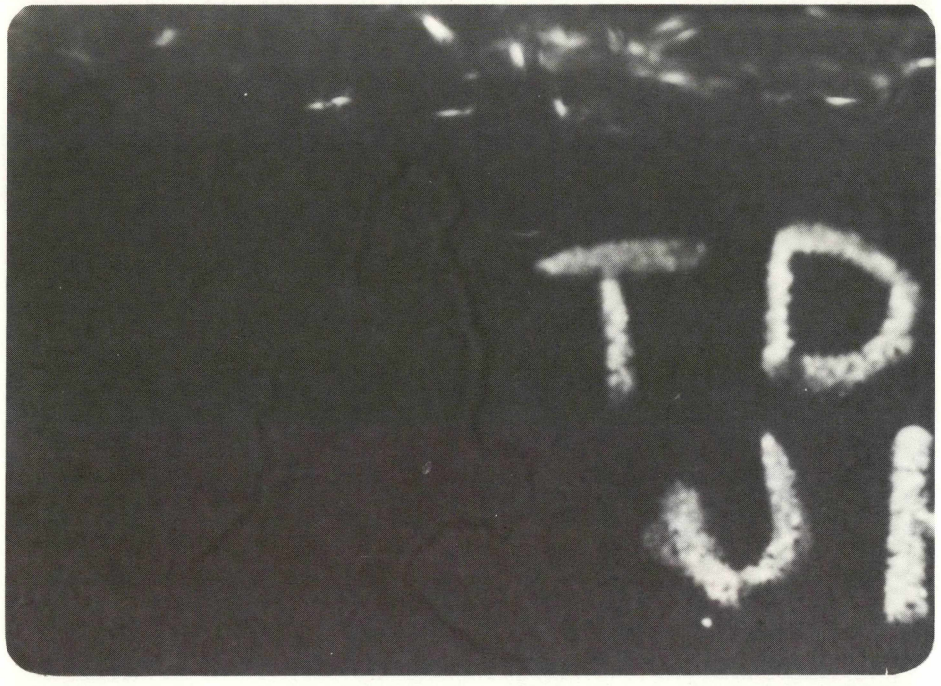

FIGURE A-4. MAGNETIC PARTICLE PATTERN OF TRANSVERSE DEFECT UNDER AN ENGINE BURN IN RAIL JK

Magnetic particle inspection techniques were applied in rail section EF to numerous engine burns, flaws which are not classified by AAR as harmful defects. Seven of the twelve such burns checked nonetheless gave pattern indications for subsurface flaws which had broken through to the surface. The cracks were not visible to the naked eye, however. Similarly, several other selected flaws (transverse fissures, compound fissures, and a transverse defect under an engine burn) in other rail sections were also inspected with magnetic particles. Few of these latter flaws gave a surface indication, but the internal orientation of those selected was verified. In general, most transverse defects in the AAR test track did not give any surface indications by magnetic particle inspection because they were not close enough to the surface or did not break through. The locations of those such as the engine burns in rail EF noted above, however, that gave pattern indications did correlate precisely with the presence of flawlike signals noted on our previous test records.

Hand ultrasonic inspection techniques utilizing shear-wave coupling into the top of the railhead were somewhat helpful in mapping out the position and orientation of the 30 percent compound fissure in rail NO. The locations of some other transverse fissures and a detail fracture were also verified, but ultrasonics inspection was not helpful in characterizing the size and depth of these transverse defects. On the other hand, the vertical split head (VSH) defects were mapped out quite accurately using a normal-beam transducer coupling to the gauge side of the rail in both longitudinal extent and lateral position. Thus, except for the extent of the VSHs, ultrasonics inspection was unable to contribute any information as to size or depth characterization of flaws.

Figure A-3 shows the 40 percent compound fissure*, between two bolt holes, in rail IJ. Figure A-4 shows the magnetic particle indications which verify that a transverse defect under an engine burn actually broke through the rail head surface.

---

* Location also verified by ultrasonic inspection.

APPENDIX B

ELECTRODYNAMICS OF MAGNETIC RAIL INSPECTION

This appendix is an attempt to reduce some of the confusion associated with the conceptual picture of the applied magnetic field technique for rail inspection. The basic problem is to elucidate the electromagnetic mechanism producing the externally sensed signal corresponding to a material or structural variation. Although not completely general, the longitudinal magnetization of a rail by an applied magnetic field is an appropriate example for examination. This technique is illustrated in Figure B-1. When there is no relative motion between the magnet and the rail, the magnetic field near and internal to the rail is intuitively seen as a flow of flux lines. The uniformity of the field in the region of a defect, e.g., a transverse fissure, is perturbed by magnetic flux leaking from the open fissure. In this instance, an increase in the amount of flux passing through the rail is expected to produce a corresponding increase in flux leakage, and hence an increased signal fidelity and discrimination. This magnetostatic view dominated much of the early thinking about magnetic rail inspection, particularly in the Soviet Union. The question then arises as to the correctness of this magnetostatic picture when the magnet is moved relative to the rail. The economic pressures to increase the speed of inspection provided impetus for the examination of the magnetodynamic situation.

All material bodies contain electrical charges and the interaction of these electrical charges with external electrical and magnetic fields is the essence of much of modern science. In metals, these electrical charges are easily influenced by externally applied electrical and magnetic fields. Thus, the passage of the magnetic field along the rail exerts an influence of these charges, generally setting them in motion. The currents resulting from the motion of these charges are called eddy currents. The basic question is the influence of these eddy currents on the magnetostatic or quasimagnetostatic picture of flux leakage.

Minkowksi's equations are used to describe the electrodynamic behavior of moving bodies. The equations are the relativistic

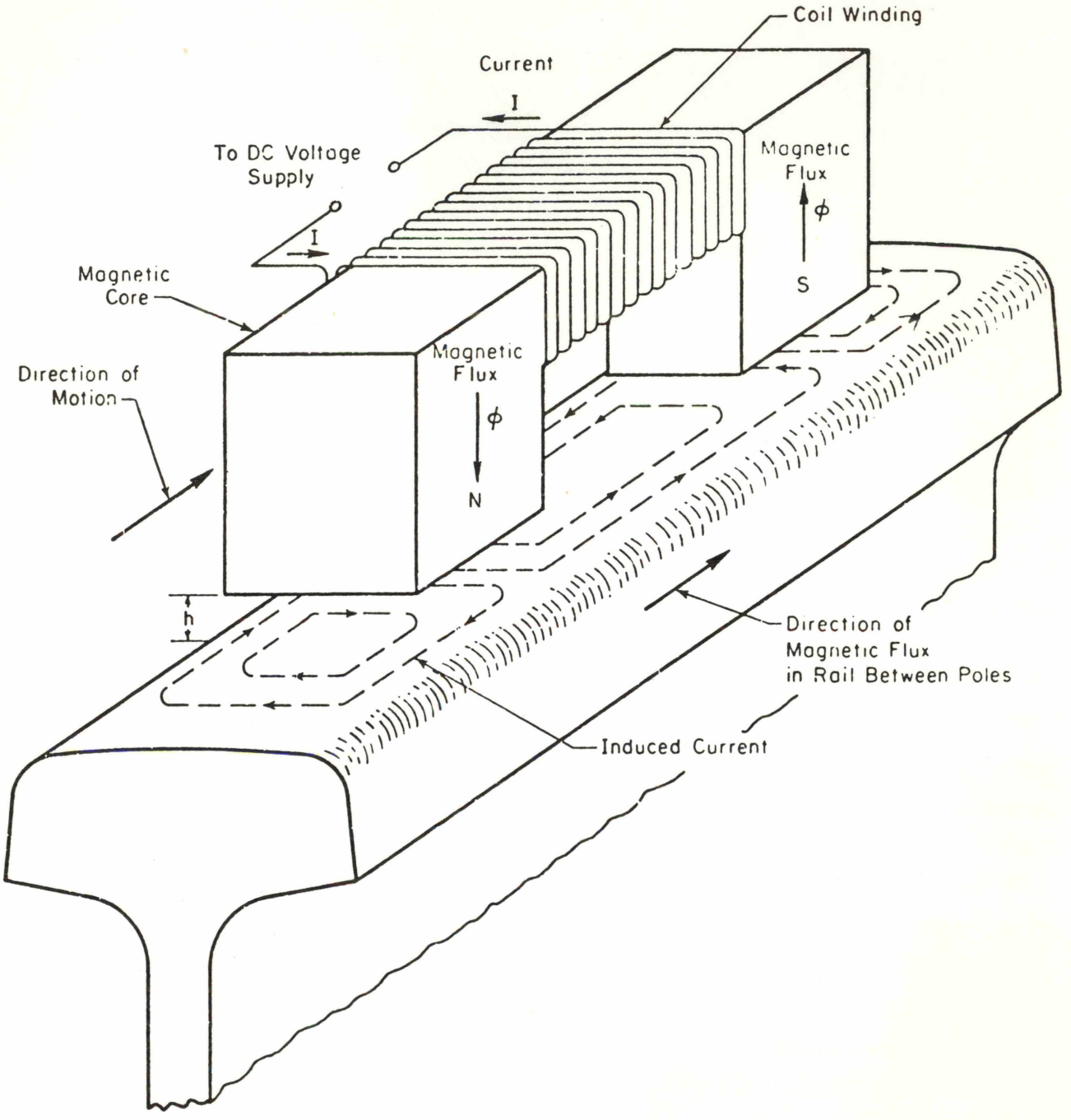

FIGURE B-1. SKETCH OF THE EDDY CURRENTS PRODUCED BY A MOVING MAGNETIC FIELD

generalization of Maxwell's equations. For speeds considerably less than the speed of light and in the absence of free charges; i.e., non-dielectrics, the Minkowski equation of importance is as follows:

$$\vec{J} = \sigma(\vec{E} + \vec{v} \times \vec{B})$$

where,

J is the current density,

σ is the conductivity,

E is the electric field,

v is the velocity,

X is the vector cross product, and

B is the magnetic induction.

The essential factor for our discussion is the $\vec{v} \times \vec{B}$ term. The physical interpretation of this form is that the induced current flow is mutually perpendicular to the direction of relative motion and the externally applied magnetic field. The magnitude of the current density is proportional to v and B.

Introduction of the magnetic vector potential reduces the above equation to an integro-differential equation whose solution requires numerical techniques for even the most idealized of cases. These mathematical difficulties were circumvented in an extensive series of experiments performed in the Soviet Union by V. V. Vlasov and his associates. Their most pertinent results were that (1) the eddy current picture dominates the field-rail interaction at speeds in considerable excess of 14 mi/h, (2) the magnetostatic picture dominates at speeds considerably less than 14 mi/h, and (3) around 14 mi/h both the magnetostatic flux leakage and eddy currents are equal contributors to the observed signals.

APPENDIX C

REPORT OF NEW TECHNOLOGY

Review of the work performed under this contract led to the discovery that sufficiently strong magnetizing fields were applied and magnetic flux sensors used to demonstrate that the longitudinal applied magnetization method of rail inspection operated successfully at speeds of approximately 25 miles per hour, with the potential of working at 40 to 50 miles per hour. A detailed description is in pages 79-84. Another payoff in the program was the discovering of successful decision processing routines such as differentiation, baseline clipping, scaling, and comparing to aid in rail flaw detection, location, and identification. Details of these processing routines are on pages 57-72. Also, a flaw characterization system was conceptualized as to the type of flaw and its general size as either small (<20%) or large (>40%), as described in pages 74-74.

☆U.S. GOVERNMENT PRINTING OFFICE: 1981 — A-2076/55

Improvement In Magnetic Techniques for Rail Inspection (Final Report), 1981
US DOT, FRA, George J Falkenbach, David J Kooger, Robert P Meister